Inflammation and Stem Cell Therapy for Stroke

Ge, Ruimin

2017

Document Version:
Publisher's PDF, also known as Version of record

Inflammation and stem cell therapy for stroke

by

Ruimin Ge

LUND
UNIVERSITY

DOCTORAL DISSERTATION
by due permission of the Faculty of Medicine, Lund University, Sweden.
To be defended at Segerfalkssalen, Wallenberg Neurocentrum, Lund, Sweden.
On June 12, 2017, at 13:00

Faculty opponent

Professor Shohreh Issazadeh-Navikas
Head of Neuroinflammation Unit, Biotech Research and Innovation Centre,
University of Copenhagen, Copenhagen, Denmark

Organization
LUND UNIVERSITY
Division of Neurology
Department of Clinical Sciences
Faculty of Medicine
Lund University, Lund, Sweden

Author(s)
Ruimin Ge

Document name
Doctoral Dissertation

Date of issue
June 12, 2017

Sponsoring organization

Title and subtitle
Inflammation and stem cell therapy for stroke

Abstract

Ischemic stroke is a leading cause of death and disability worldwide. Currently, there is no treatment that can promote recovery in the chronic phase. It has been shown that neurogenesis occurs in ischemic striatum in rodents and probably also in humans. Moreover, blood-borne macrophages have been found to enhance spontaneous post-stroke recovery in mice. These findings have suggested potential new targets to improve functional restoration after stroke.

In this thesis, we first showed that inflammation without neuronal loss is sufficient to trigger striatal neurogenesis comparable to that after stroke, indicating that inflammation might be the main inducer of post-stroke striatal neurogenesis. Using microarray on sorted microglia from subventricular zone (SVZ) and striatum, several factors were identified that potentially could regulate different steps of striatal neurogenesis after stroke. Some of the identified factors have previously been reported to regulate neural stem/progenitor cells (NSPC) proliferation or differentiation. We examined in some detail one factor, Cxcl13, and found that it promotes neuroblasts migration in *vitro*. Next, we provided evidence that monocyte-derived macrophages (MDM) can take the choroid plexus (CP)-cerebrospinal fluid (CSF) route for infiltration into the brain after cortical stroke. We found that *in vitro*-derived anti-inflammatory (M2-like) MDM delivered into CSF migrate into ischemic cortex, maintain their M2-like phenotype, and most importantly, improve recovery of motor and cognitive function in stroke-subjected mice without influencing infarct volume. These findings highlight the crucial role of inflammatory cells, such as microglia and macrophages, in post-stroke cellular plasticity and functional recovery.

We also explored another approach for cell delivery into the brain using human induced pluripotent stem cells (iPSC)-derived long-term neuroepithelial-like stem (lt-NES) cells. Following our previous findings that transplantation of these cells and their derivatives promotes post-stroke motor function recovery, we showed that stroke influences the migration and axonal projection pattern of iPSC-derived lt-NES cells implanted adjacent to the neurogenic SVZ. These data indicate that the occurrence of ischemic injury strongly affects crucial parameters in the behavior of transplanted neural progenitors, which will be important to consider in a potential, future clinical translation. Finally, by combining immunoelectron microscopy, rabies virus-based trans-synaptic tracing, *in vivo* electrophysiological recordings and optogenetic techniques, we for the first time showed that neurons derived from transplanted iPSC-derived lt-NES cells receive functional synaptic inputs from host neurons located in the appropriate brain areas, e.g. ventral thalamus, after stroke. We demonstrated that tactile stimulation of nose and paws can activate or inhibit spontaneous activity in grafted neurons, providing evidence that that they can become incorporated into injured cortical circuitry. Since we have found that transplanted M2-like MDM promote post-stroke recovery, possibly by modulating neuronal circuit plasticity, it seems highly warranted to examine whether delivery of M2-like MDM would further enhance the integration of neurons generated from grafted iPSC-derived lt-NES cells in the stroke model.

Taken together, our findings raise the possibility that modulation of inflammatory mechanisms, delivery of M2-like MDM and transplantation of neurons generated from iPSC-derived lt-NES cells might become of value in future therapeutic approaches for improved functional recovery in stroke patients.

Key words
Inflammation, Ischemic stroke, Neurogenesis, Choroid plexus, M2-like macrophages, Microglia, Neuroepithelial-like stem cells, Transplantation, Neuronal integration

Classification system and/or index terms (if any)

Supplementary bibliographical information

Language

ISSN and key title
1652-8220

ISBN
978-91-7619-488-1

Recipient's notes

Number of pages
150

Price

Security classification

Inflammation and stem cell therapy for stroke

by

Ruimin Ge

LUND
UNIVERSITY

Coverphoto by Ruimin Ge and Bengt Mattsson:

In the middle of the cover, there is the traditional Chinese Wuxing (Five elements) model. This model describes the interactions among five elements: Water, Wood, Fire, Earth and Metal. The interactions can be either promotion/generation (yellow arrow), or inhibition/elimination (red arrow). This model reflects very well the promotional or inhibitory interactions among different cells in the human body. The three surrounding cartoons represent pro-inflammatory M1/anti-inflammatory M2 microglia/macrophage (upper), neurogenesis (lower left), and sprouting neuron (lower right). Together with the Wuxing model, the cartoons show the main topic of the thesis: interactions among inflammation represented by activation of microglia/macrophages, sprouting of neurons and neurogenesis (either from endogenous or transplanted neural stem cells) in the brain affected by ischemic stroke.

ISSN 1652-8220
ISBN 978-91-7619-488-1
Lund University, Faculty of Medicine Doctoral Dissertation Series 2017:106

Printed in Sweden by Media-Tryck, Lund University
Lund 2017

Content

Original papers

1. Chapman K.Z*, **Ge R***, Monni E, Tatarishvili J, Ahlenius H, Arvidsson A, Ekdahl CT, Lindvall O, Kokaia Z. Inflammation without neuronal death triggers striatal neurogenesis comparable to stroke. ***Neurobiology of Disease***, 2015, 83, 1-15. DOI: 10.1016/ j.nbd.2015.08.013. *(*Equal contribution)*

2. **Ge R**, Tornero D, Hirota M, Monni E, Lindvall O, and Kokaia Z. Choroid Plexus-Cerebrospinal Fluid Route for Beneficial Monocyte-Derived Macrophages After Stroke. (***Submitted***, Track ID: JNEU-D-17-00151)

3. Rosa-Prieto C, Laterza C, Gonzalez-Ramos A**,** Wattananit S, **Ge R**, Lindvall O, Tornero D and Kokaia Z. Stroke Alters Behavior of Human Skin-Derived Neural Progenitors after Transplantation Adjacent to Neurogenic Area in Rat Brain. ***Stem Cell Research & Therapy***, 2017, 8:59. DOI: 10.1186/s13287-017-0513-6.

4. Tornero D, Tsupykov O, Granmo M, Rodriguez C, Grønning-Hansen M, Thelin J, Smozhanik E, Laterza C, Wattananit S, **Ge R**, Tatarishvili J, Grealish S, Brüstle O, Skibo G, Parmar M, Schouenborg J, Lindvall O and Kokaia Z. Synaptic inputs from stroke-injured brain to grafted human stem cell-derived neurons activated by sensory stimuli. ***Brain***, 2017, 140 (3): 692-706. DOI: 10.1093/brain/aww347.

Summary

Ischemic stroke is a leading cause of death and disability worldwide. Currently, there is no treatment that can promote recovery in the chronic phase. It has been shown that neurogenesis occurs in ischemic striatum in rodents and probably also in humans. Moreover, blood-borne macrophages have been found to enhance spontaneous post-stroke recovery in mice. These findings have suggested potential new targets to improve functional restoration after stroke.

In this thesis, we first showed that inflammation without neuronal loss is sufficient to trigger striatal neurogenesis comparable to that after stroke, indicating that inflammation might be the main inducer of post-stroke striatal neurogenesis. Using microarray on sorted microglia from subventricular zone (SVZ) and striatum, several factors were identified that potentially could regulate different steps of striatal neurogenesis after stroke. Some of the identified factors have previously been reported to regulate neural stem/progenitor cells (NSPC) proliferation or differentiation. We examined in some detail one factor, Cxcl13, and found that it promotes neuroblasts migration in *vitro*. Next, we provided evidence that monocyte-derived macrophages (MDM) can take the choroid plexus (CP)-cerebrospinal fluid (CSF) route for infiltration into the brain after cortical stroke. We found that *in vitro*-derived anti-inflammatory (M2-like) MDM delivered into CSF migrate into ischemic cortex, maintain their M2-like phenotype, and most importantly, improve recovery of motor and cognitive function in stroke-subjected mice without influencing infarct volume. These findings highlight the crucial role of inflammatory cells, such as microglia and macrophages, in post-stroke cellular plasticity and functional recovery.

We also explored another approach for cell delivery into the brain using human induced pluripotent stem cells (iPSC)-derived long-term neuroepithelial-like stem (lt-NES) cells. Following our previous findings that transplantation of these cells and their derivatives promotes post-stroke motor function recovery, we showed that stroke influences the migration and axonal projection pattern of iPSC-derived lt-NES cells implanted adjacent to the neurogenic SVZ. These data indicate that the occurrence of

ischemic injury strongly affects crucial parameters in the behavior of transplanted neural progenitors, which will be important to consider in a potential, future clinical translation. Finally, by combining immunoelectron microscopy, rabies virus-based trans-synaptic tracing, *in vivo* electrophysiological recordings and optogenetic techniques, we for the first time showed that neurons derived from transplanted iPSC-derived lt-NES cells receive functional synaptic inputs from host neurons located in the appropriate brain areas, e.g. ventral thalamus, after stroke. We demonstrated that tactile stimulation of nose and paws can activate or inhibit spontaneous activity in grafted neurons, providing evidence that they can become incorporated into injured cortical circuitry. Since we have found that transplanted M2-like MDM promote post-stroke recovery, possibly by modulating neuronal circuit plasticity, it seems highly warranted to examine whether delivery of M2-like MDM would further enhance the integration of neurons generated from grafted iPSC-derived lt-NES cells in the stroke model.

Taken together, our findings raise the possibility that modulation of inflammatory mechanisms, delivery of M2-like MDM and transplantation of neurons generated from iPSC-derived lt-NES cells might become of value in future therapeutic approaches for improved functional recovery in stroke patients.

Abbreviations

Arg1	Arginase-1
BrdU	5-Bromo-2-deoxyuridine
BSA	Bovine serum albumin
ChR2	Channelrhodopsin-2
CNS	Central nervous system
CP	Choroid plexus
CSF	Cerebrospinal fluid
Cxcl12	C-X-C motif chemokine ligand 12
Cxcl13	C-X-C motif chemokine ligand 13
Cx_3cl1	C-X3-C motif chemokine ligand 1
Cx_3cr1	C-X3-C chemokine receptor 1
Cxcr5	C-X-C chemokine receptor 5
DAB	3,3'-diaminobenzidine tetrahydrochloride
DAMP	Danger-associated molecular pattern
DCX	Doublecortin
dMCAO	permanent distal branch middle cerebral artery occlusion
ED1	Macrosialin (CD68)
ESC	Embryonic stem cells
FACS	Fluorescent-activated cell sorting
FBS	Fetal bovine serum
GAD65/67	65/67 kDa glutamic acid decarboxylase
Gaphd	Glyceraldehyde-3-phosphate dehydrogenase
GFAP	Glial fibrillary acidic protein
GFP	Green fluorescent protein
Hprt	Hypoxanthine-guanine phosphoribosyl transferase
Iba1	Ionized calcium-binding adapter molecule 1, Allograft inflammatory factor 1(Aif-1)
ICA	Internal carotid artery
IFNγ	Interferon gamma

IGF1	Insulin-like growth factor 1
IL1β	Interleukin-1 beta
IL4	Interleukin-4
IL6	Interleukin-6
IL13	Interleukin-13
IL15	Interleukin-15
iNOS	inducible nitric oxide synthase
iPSC	induced pluripotent stem cells
LPS	Lipopolysaccharide
lt-NES cells	long-term neuroepithelial-like stem cells
Madcam1	Mucosal addressin cell adhesion molecule 1
MCA	Middle cerebral artery
MCAO	Middle cerebral artery occlusion
MCP1	Monocyte chemoattractant protein 1, C-C motif chemokine ligand 2 (Ccl2)
MDM	Monocytes derived macrophages
MOB	Main olfactory bulb
NeuN	Neuronal nuclei antigen
NSPC	Neural stem/progenitor cells
Nt5e	5'-Nucleotidase
PBS	Phosphate-buffered saline
PDGFRα	Platelet-derived growth factor receptor alpha
PFA	Paraformaldehyde
PSA-NCAM	Polysialylated neuronal cell adhesion molecule
RMS	Rostral migratory stream
ROS	Reactive oxygen species
SVZ	Subventricular zone
Tgfβ1	Transforming growth factor beta-1
TNFα	Tumor necrosis factor alpha
Vcam1	Vascular cell adhesion molecule 1
Ym1	Beta-N-acetylhexosaminidase, Chitinase-like protein 3 (chil3)

Introduction

Ischemic stroke, which represents more than 85% of all stroke cases, is a leading cause of death and disability worldwide. It is commonly caused by occlusion of blood flow to a certain brain area due to *in situ* thrombosis or embolism. Currently, the only clinically proven treatments for ischemic stroke are thrombolysis and thrombectomy, which restore blood flow to the ischemic area. However, these treatments can only be applied within the first 6 h after the initial attack. Thus, only a minority of patients benefit from these therapies. There is no available treatment that can promote recovery in the chronic phase after ischemic stroke.

Regenerative processes after ischemic stroke

Our laboratory for the first time showed that neuroblasts generated from neural stem/progenitor cells (NSPC) in subventricular zone (SVZ) migrate to the ischemic area in the striatum and differentiate to neurons in a rat stroke model (Arvidsson et al., 2002). This process lasted for several months after the insult and still occurred in aged animals at the same level as in young ones (Darsalia et al., 2005; Thored et al., 2006). Depletion of DCX+ neuroblasts in mice has been reported to worsen the ischemic damage and motor behavioral deficit after stroke, suggesting that neurogenesis may be beneficial for post-stroke outcome (Jin et al., 2010). There is evidence that the newly formed neurons can be functionally integrated into existing neuronal circuitry in the striatum after stroke (Hou et al., 2008). Interestingly, neurogenesis seems to occur also in stroke patients (Marti-Fabregas et al., 2010; Minger et al., 2007). Recently, it was found that astrocytes in the striatum can convert to neuroblasts and differentiate to mature neurons after stroke (Magnusson et al., 2014), acting as another source for striatal neurogenesis besides NSPC in the SVZ after stroke.

Reactive gliosis occurs after injury in the adult CNS. Formation of the glial scar could limit the inflammatory response and reduce damage after injury, but also hinder axonal growth in the chronic phase (Robel et al., 2011; Silver and Miller, 2004). Degradation or blockage of axonal growth inhibitory molecules, such as chondroitin sulfate proteoglycan,

NogoA and Myelin-associated glycoprotein, has been shown to increase neurite growth and improve recovery after stroke (Cash et al., 2016; Hill et al., 2012; Lindau et al., 2014). In the peri-infarct cortex outside the glia scar, new patterns of intracortical projections were identified (Carmichael et al., 2001), and factors such as growth and differentiation factor 10 are expressed that can enhance axonal growth and promote recovery (Carmichael et al., 2005; Li et al., 2015). Moreover, there is evidence that cortical reorganization underlies the motor function recovery observed in stroke patients (Hodics et al., 2006; Schaechter et al., 2002). Taken together, these data highlighted that it might be possible to promote post-stroke recovery by enhancing axonal growth and functional plasticity of remaining neuronal circuitry.

Inflammation after ischemic Stroke

When a brain area is deprived of nutrients and oxygen due to occlusion of blood flow in ischemic stroke, neurons in the infarct core die rapidly within seconds to minutes, while neurons in the surrounding penumbra can survive for a few hours (Moskowitz et al., 2010). Various danger-associated molecular pattern (DAMP) released from the dead neurons activate the immune system, triggering resident microglia activation and then blood-borne leukocyte infiltration (Iadecola and Anrather, 2011). These inflammatory cells can exacerbate brain injury by releasing inflammatory mediators such as ROS and various pro-inflammatory cytokines in the early phase. Infiltrating polymorphonuclear leukocytes could also occlude capillaries following reperfusion after ischemic stroke (del Zoppo et al., 1991). Despite the elucidated harmful effect of inflammatory cells after stroke, several compounds targeting these cells were proven ineffective in stroke patients. Enlimomab, an anti-intercellular adhesion molecule-1 (ICAM-1) antibody that reduces leukocyte adhesion, significantly worsens outcome in stroke patients (Enlimomab Acute Stroke Trial Investigators, 2001). The UK-279276, a neutrophil inhibitory factor, shows no effect in improving recovery in stroke patients (Krams et al., 2003). Therefore, the role of inflammation in stroke needs further exploration.

Several microglia/macrophage-derived factors have been identified to regulate different steps of striatal neurogenesis after stroke. IGF1 and IL15 have been shown to

promote NSPC proliferation in SVZ (Gomez-Nicola et al., 2011; Thored et al., 2009; Yan et al., 2006), while CXCL12 and MCP1 were found to mediate neuroblasts migration to the injured area after stroke (Robin et al., 2006; Yan et al., 2007). Microglia and blood-borne macrophages can reside in different states, expressing different markers, releasing various cytokines, and having diverse biological functions (Gordon and Taylor, 2005; Mantovani et al., 2013). Classically activated M1-like macrophages, induced by IFNγ, are pro-inflammatory by releasing ROS and inflammatory cytokines such as IL1β, TNFα and IL6. In contrast, alternatively activated M2-like macrophages, induced by IL4 and IL13, are involved in dampening inflammation and promotion of tissue remodeling (Mantovani et al., 2013). It was recently found that after ischemic stroke, blood-borne macrophages switch from M1- to M2-like in mice subjected to middle cerebral artery occlusion (MCAO) (Miro-Mur et al., 2016; Wattananit et al., 2016). The M1-like microglia inhibited while M2-like microglia promoted neuronal survival in hypoxic conditions *in vitro* (Hu et al., 2012). Moreover, blood-borne macrophages were found to be essential for recovery after ischemic stroke, possibly by enhancing axonal growth or plasticity of existing neuronal circuitry (Wattananit et al., 2016).

Stem cell therapy for ischemic stroke

The existence of neurogenesis in the ischemia area (Arvidsson et al., 2002), and the finding of axonal growth-promoting environment in the peri-infarct cortex (Carmichael et al., 2005), raise the possibility that it might be possible to transplant NSPC and their derivatives into the area around the ischemia, where they could differentiate to neurons, which become incorporated into reorganizing host neural circuitry. Human fetal NSPC can survive, migrate and differentiate to neurons after transplantation into ischemic striatum or cortex of rats subjected to stroke (Darsalia et al., 2007; Kelly et al., 2004), and could improve functional recovery after stroke (Ishibashi et al., 2004; Mine et al., 2013). NSPC derived from human embryonic stem cells (ESC) could also survive and improve functional recovery after transplanted into ischemic rat brain (Daadi et al., 2008; Kim et al., 2007). In human stroke patients, intracerebral transplantation of immortalized human NSPC showed no adverse effect and was associated with improved neurological function

(Kalladka et al., 2016). Transplantation of stem cells other than NSPC to treat stroke has also been explored. Bone marrow-derived mesenchymal stem cells were shown to ameliorate neurological deficit after transplanted into cortex surrounding ischemic area in rats (Zhao et al., 2002), and transplantation of autologous or nonautologous bone marrow stem cells into stroke patients, either intravenously or intraparenchymally into the peri-lesion area, has been reported safe (Hess et al., 2017; Honmou et al., 2011; Steinberg et al., 2016; Suarez-Monteagudo et al., 2009). Human cord-blood derived CD34+ endothelial progenitor cells administered systemically were found to promote neurogenesis and angiogenesis in mice stroke model (Taguchi et al., 2004). However, these stem cells do not have the potential to differentiate to neurons and replace the neurons lost due to ischemic damage.

Generation of large numbers of NSPC for possible transplantation to stroke patients has been a problem. The use of human ESC to generate NSPC is associated with ethical problems. In 2006, it was found that induced pluripotent stem cells (iPSC) could be generated from adult fibroblasts by defined factors (Takahashi et al., 2007). Later, various laboratories have developed protocols to differentiate iPSC to different cell types including neurons (Kim et al., 2011). These findings raise the possibility that neurons for transplantation could be generated from the stroke patients' own fibroblasts. We have previously found that human iPSC-derived lt-NES cells, primed to a cortical neuronal fate, can promote post-stroke motor recovery after transplantation into cortex surrounding the ischemic area (Tornero et al., 2013). However, whether neurons generated from iPSC-derived lt-NES cells receive functional synaptic inputs from host neurons is unknown.

In this thesis, we have investigated the role of inflammation in post-stroke striatal neurogenesis. We have also explored the role of choroid plexus (CP) in mediating infiltration of MDM into the brain after ischemic stroke and the possibility of promoting post-stroke recovery by enhancing M2-like MDM infiltration via CSF. We then examined the effect of stroke on the behavior of transplanted human iPSC-derived lt-NES cells. Finally, we analyzed the synaptic input from host neurons on transplanted neurons generated from transplanted iPSC-derived lt-NES cells after stroke.

Aims of the thesis

The main aims of the studies included in present thesis were as follows:

1. To explore whether the injury *per se* or the associated inflammation induces striatal neurogenesis after stroke

2. To elucidate the role of CP in recruiting MDM, especially beneficial M2-like MDM, to the injured brain after stroke

3. To analyze the effect of the ischemic injury on the behavior of human iPSC-derived lt-NES cells transplanted adjacent to a neurogenic area after stroke

4. To determine if grafted neurons, generated from human iPSC-derived lt-NES cells and implanted in the stroke-injured cortex, receive functional synaptic inputs from the host brain and respond to physiological sensory stimuli

Materials and Methods

Animals

All procedures were carried out in accordance with the guidelines set by the Malmö-Lund Ethical Committee for the use of laboratory animals, and were conducted in accordance with the European Union directive on the subject of animal rights. Procedures were carried out on male Wistar rats (250-300 g, Charles River, Germany), male nude rats (250-300 g, Charles River, Germany), male C57BL/6 mice (25-30g, Charles River, Germany), male Cx_3cr1^{GFP} mice (25-30 g, The Jackson Laboratory stock No. 005582), and male $CXCR5^{-/-}$ mice (25-30 g, The Jackson Laboratory stock No. 006659), housed under 12 h light/12 h dark cycle with *ad libitum* access to food and water.

Surgical Procedures

Animals were anaesthetized with isoflurane (3.0% induction; 1.5% maintenance) mixed with air. All animals received locally injected marcaine for pain relief. While under anaesthesia and in the early recovery period (2 h), animals were placed on a heating pad at 37°C.

Lipopolysaccharide (LPS) from *Salmonella enterica*, serotype *abortusequi* (Sigma-Aldrich; 15 µg in 1.5 µl of artificial CSF (aCSF)) or vehicle (aCSF) was stereotaxically injected using a self-made glass microneedle fixed to a gas-tight syringe (Hamilton) into the right striatum (coordinates: 1.2 mm rostral, 2.5 mm lateral to bregma, 4.5 mm ventral from brain surface, tooth bar at -3.3 mm). In a pilot experiment in mice, a dose-response curve was established with 0.01 to 100 µg LPS administered in ten-fold increasing concentrations as above (coordinates: 0.9 mm rostral, 1.6 mm lateral to bregma and 3.5 mm ventral from brain surface, tooth bar at 0 mm).

The intraluminal filament technique was used to induce transient middle cerebral artery occlusion (MCAO). In rats, the right carotid arteries were isolated and the common and external carotid arteries were proximally ligated. The internal carotid artery (ICA) was temporarily occluded with a microvascular clip. A small incision was made in the

common carotid artery and a heat-blunted nylon microfilament was advanced into the ICA until resistance was felt (approx. 19 mm). Animals recovered from anesthesia during the occlusion. 30 min after occlusion, animals were re-anesthetized and the filament was withdrawn. Temperature was maintained at 37 ± 0.5 °C while animals were under anesthesia. Sham surgeries were carried out in the same way but the filament was only advanced 2 mm inside the ICA. The MCAO-subjected animals that did not fulfill pre-defined inclusion criteria for successful 30 min occlusion (> 40% striatal damage; no cortical damage; no subarachnoid hemorrhage) were excluded following NeuN staining. In mice, the procedure was modified as follows: right carotid arteries were isolated, and the common carotid artery and the external carotid artery were ligated. The ICA was temporarily occluded with a microvascular clip, and a silicon-coated microfilament was placed into the external carotid artery via a small incision and advanced into the ICA until resistance was felt (approx. 9 mm). Occlusion was maintained for 35 min before the filament was withdrawn.

The distal MCAO (dMCAO) was performed on adult 25-30g C57BL/6 mice under anesthesia as described elsewhere (Perez-de Puig et al., 2013). In brief, after shaving the skin, a scission was made between the right eye and the right ear. Muscles covering the cranium were cut and opened, and a small hole was then drilled in the cranium at the level of the distal portion of the right MCA. The dura mater was removed and the artery was visualized and occluded by cauterization. The artery was then cut off to make sure there was no remaining blood flow to the corresponding cortical region. After the skin had been sutured, mice were injected with 1.5 ml Ringer's solution, returned to their cages and put on a heating pad. For sham-operated mice, the distal portion of the MCA was exposed in the same way as in dMCAO surgery, but without occlusion of the artery using cauterization. For dMCAO surgery on rats, branch of MCA was dissected in the same way as in mice, but was occluded with suture rather than cauterization. Also, both common carotid arteries were isolated and temporarily ligated for 30 min after MCAO. Following release of common carotid arteries, surgical wounds were closed.

For macrophages transplantation, phosphate-buffered saline (PBS) solutions with or without cells were stereotaxically injected using a glass microneedle into the lateral ventricle (coordinates: 0.1 mm rostral, 1.0 mm lateral to bregma, 2.2 mm ventral from

brain surface). Injection was carried out 1 day after MCAO. Mice were randomly allocated to Cell or PBS (vehicle) groups using a random sequence generated (https://www.random.org). In total 5 µl PBS with or without 3 million cells were injected with speed 1 µl/min. Microneedle was left in place for 5 min after all solution had been injected, and was then slowly removed during 1 min. Finally, wound was cleaned and sutured, and mice were returned to cages with heating pads.

Intracortical transplantation of lt-NES cells, which had been transduced with lentivirus carrying green fluorescent proten (GFP) (for *in vivo* tracing, immunoelectron microscopy, *in vivo* electrophysiological recording and optogenetic experiments) or with tracing vector (for monosynaptic tracing experiments), was performed stereotaxically at 48 h after dMCAO. On the day of surgery, cortically primed cells in the seventh day of differentiation were resuspended to a final concentration of 100 000 cells/µl. A volume of 1.5 µl was injected at two sites (coordinates 1: 0.5 mm rostral, 1.5 mm lateral to bregma, 2.5 mm ventral from brain surface; coordinates 2: 1.5 mm rostral, 1.5 mm lateral to bregma, 2.0 mm ventral from brain surface). For lt-NES cells transplantation into rostral migratory stream (RMS), a volume of 2 µl of cells was injected at the following coordinates: 1.8 mm rostral, 1.7 mm lateral to bregma, 4.0 mm ventral from brain surface with tooth bar set at - 3.3mm. Sprague-Dawley rats were given Cyclosporine A 10 mg/kg subcutaneously every day during the first month and every other day during the second month after transplantation.

Monocyte isolation

Bone marrow cells were collected from male Cx3cr1^{GFP} or wildtype C57BL/6 donor mice by crushing the femurs, tibiae, and hips. Cells were passed through a 40 µm strainer and rinsed with PBS supplemented with 2% fetal bovine serum (FBS). CD115+ cells were isolated using a magnetic cell separation system and biotinylated anti-CD115 antibody combined with streptavidin-magnetic beads (Miltenyi Biotec, Germany). The freshly isolated monocytes were used for direct transplantation or further culture.

Choroid plexus tissue and cerebrospinal fluid collection

For choroid plexus (CP) tissue collection, mice were deeply anaesthetized with an overdose of pentobarbital and transcardially perfused with at least 150 ml 4°C saline to thoroughly remove blood from CP. Brain was removed and CP tissues were collected under surgical microscope. The CP in the 4th ventricle was first collected, followed by the ones in 3rd and lateral ventricles. The CP tissues were then transferred into pre-cooled Eppendorf tube on dry ice for RNA collection or in 4°C L-15 medium for fluorescent-activated cell sorting (FACS) analysis. For immunohistochemical analysis of CP, freshly isolated tissue was fixed in 4% paraformaldehyde (PFA) overnight and washed in PBS for further analysis.

The CSF was collected from cisterna magna (Liu and Duff, 2008). In brief, mice were anaesthesized using isoflurane (3.0% induction; 1.5% maintenance) mixed with air, and were then fixed on a stereotaxic frame. A scission over the back of the neck was made, and muscles covering cisterna magna were separated using a pair of cotton anti-bleeding bars. Body of the mouse was bent at 135° to the head. Cisterna magna was visualized under microscope. A glass pipette was carefully inserted into cisterna magna with avoidance of *arteria spinalis dorsalis*. On average, 2 μl of CSF was collected from each mouse. Any CSF contaminated with blood was discarded. The collected CSF was blown out from the glass pipette using a syringe, and was kept at 4°C for further analysis.

Immunohistochemistry

Animals were deeply anaesthetized with an overdose of pentobarbital and transcardially perfused with saline followed by 4% PFA. Brains were post-fixed overnight in 4% PFA and then placed in 20% sucrose for 24 h before coronal sectioning (30 μm) with freezing microtome.

All sections for BrdU staining were pre-treated with 1 M HCl for 10 min at 65°C and 20 min at room temperature. All stains were carried out according to the following protocol: free-floating sections were pre-incubated with the appropriate serum and then incubated with primary antibodies overnight at 4°C. Sections were incubated for 2 h in the dark with Cy3, Alexa Fluor 488, or Alexa Fluor 647 (1:200, Molecular Probes, Life

Technologies) conjugated secondary donkey anti-rat/goat/rabbit/mouse/chicken (all 1:200, Jackson ImmunoResearch), or biotinylated horse anti-mouse/goat (both 1:200, Vector Laboratories) antibodies. Nuclei were stained with Hoechst 33342 (1:4000, Molecular Probes or Jackson Laboratories) for 10 min followed by three rinses and sections were mounted with Dabco (Sigma) on gelatin-coated slides. The primary antibodies were as follows:

Antibody	**Host species**	**Concentration**	**Company**
Anti-BrdU	Rat	1:200	Abcam
Anti-NeuN	Mouse	1:100	Merck Millipore
Anti-NeuN	Rabbit	1:2000	Abcam
Anti-DCX	Goat	1:400	Santa Cruz Biotechnology
Anti-Iba1	Rabbit	1:1000	Wako
Anti-ED1	Rat	1:200	AbDSerotec
Anti-ki67	Mouse	1:500	Novocastra, Leica Biosystems
Anti-HuD	Rabbit	1:200	Sigma
Anti-S100β	Rabbit	1:200	Sigma
Anti-GFAP	Rabbit	1:400	Zymed, Life Technologies
Anti-GFAP	Mouse	1:500	Stem Cells
Anti-nestin	Mouse	1:200	Merck Millipore
Anti-CD16/32	Rat	1:200	BD Biosciences
Anti-iNOS	Rabbit	1:200	BD Biosciences
Anti-RECA	Mouse	1:400	AbDSerotec
Anti-CD206	Goat	1:100	R&D
Anti-YM1	Rabbit	1:100	Abcam
Anti-GFP	Chicken	1:3000	Millipore
Anti-GFP	Goat	1:1000	Abcam
Anti-PDGFRα	Mouse	1:300	Santa Cruz Biotechnology
Anti-SC101	Mouse	1:200	Stem Cells
Anti-SC121	Mouse	1:400	Stem Cells

Anti-mCherry	Rabbit	1:500	Abcam
Anti-Calretinin	Goat	1:1000	Millipore
Anti-Calbindin	Rabbit	1:500	Sigma
Anti-Calretinin	Goat	1:1000	Millipore
Anti-Parvalbumin	Mouse	1:5000	Swant Inc
Anti-KGA	Rabbit	1:200	Abcam
Anti-GAD65/67	Rabbit	1:400	Sigma

Single labeling for NeuN was performed with biotinylated horse anti-mouse or anti-rabbit antibody and visualized with avidin-biotin-peroxidase complex (Elite ABC kit, Vector Laboratories), followed by peroxidase-catalyzed diaminobenzidine reaction.

Microscopical analysis

All microscopical analysis and quantifications were performed by investigator being blinded to treatment conditions.

Neuronal death was assessed by an estimation of the total number of remaining NeuN+ cells in the striatum using the Optical Fractionator method (West et al., 1991). This was carried out using the Computer Assisted Stereological Toolbox (C.A.S.T-GRID) software (Olympus, Denmark) with sampling from three coronal sections at approximately 0.9 mm, 1.2 mm (LPS injection site) and 1.5 mm rostral from Bregma. In brief, images from the microscope were acquired with a digital camera and displayed live on a monitor screen. Using a 1.25 x objective, the striatum was delineated on the screen according to pre-defined criteria: dorsal and lateral boundaries along the corpus callosum and the medial sides of claustrum and dorsal endopiriform nucleus; ventral boundary along a line drawn from the border of the dorsal endopiriform nucleus at the level of the flexure of the piriform cortex to the anterior commissure, or at more caudal levels along a line following the posterior part of the anterior commissure; and the medial boundary along a line drawn from the anterior commissure to the ventral tip of the lateral ventricle and the lateral side of the ventricle, or at more caudal levels along the lateral side of globus pallidus and the lateral side of the lateral ventricle. The thickness of each section

was measured at high magnification at multiple locations within the delineated striatum using a microcator attached to the stage of the microscope. The striatum was then systematically sampled at high magnification and cells at each sampling point were counted using a three-dimensional probe (counting frame combined with optical dissector) following accepted stereological cell counting methods. Counting frame area and stepping distances were chosen to sample 100-200 cells per striatum, keeping the number of cells counted at each sampling point as close to 1 as possible. Number of cells per striatum was calculated by dividing the number of cells counted with the sampling fraction. Images of SVZ in sections with NeuN and cresyl violet staining from the same aforementioned rostro-caudal levels were first taken under 40 x magnification. The SVZ was then defined by cells stained only with cresyl violet and area was measured using Visiopharm software (Visiopharm, Denmark). For volume measurement, striatum was first delineated using the pre-defined criteria as described above. Area was then measured using Visiopharm software (Visiopharm, Denmark) in coronal sections from +2.2 mm to -0.4 mm from bregma. Striatal volume was estimated by multiplying the areas with the distance between sections (240 μm). Numbers of Iba1+, BrdU+/DCX+, BrdU-/DCX+, BrdU+/NeuN+ single or double-labeled cells in the rat striatum were counted using a 0.0625 mm^2 quadratic grid on an epifluorescence microscope with a 40 x objective on the three coronal sections described above. Cell counts are presented as the total number in these 3 sections. Because striatal volume was decreased in MCAO animals (by 20% and 38% at 2 and 6 weeks after the insult, respectively, compared to sham groups), the NeuN +, Iba1+, BrdU+/DCX+, BrdU-/DCX+ and BrdU+/NeuN+ cell counts in 3 coronal sections were, therefore, multiplied with the shrinkage ratio to compensate for the effect of shrinkage on cell density. The shrinkage ratio was calculated by dividing Iba1+ cell density in all striatal sections (2.2 mm rostral to 0.4 mm caudal from bregma) with Iba1+ cell density in the 3 coronal sections (0.9 mm, 1.2 mm and 1.5 mm rostral from bregma). Distribution of cells was calculated as described previously (Thored et al., 2006). Additionally, 50 DCX+ cells per animal were analyzed using epifluorescence microscopy to assess co-expression with HuD, PDGFRα or S100β.

Since it was not feasible to count astrocyte numbers due to the extensive astrogliosis seen in both MCAO and LPS-injected animals, each animal was given a score of 0-3 by a

blinded observer based on a semi-quantitative scale of astrocyte activation as observed by GFAP and nestin staining: Score 0: astrocytes appear branched and thin with no aggregation; no nestin+/GFAP+ cells; no obvious increase in astrocyte numbers compared to contralateral side. Score 1: some astrocytes exhibit a more swollen, 'active' phenotype but with minimal aggregation; active astrocytes are limited to less than 1/3 of striatum with only small increase in numbers; less than 1/3 of 'active' GFAP+ cells are nestin+. Score 2: astrocytes exhibit 'active' phenotype and aggregation, with clear increase in numbers; more than 1/3 but less than 2/3 of 'active' GFAP+ cells are nestin+; activation localized or more diffuse. Score 3: astrocytes exhibit 'active' phenotype and aggregation, with clear increase in numbers; more than 2/3 of 'active' GFAP+ cells are nestin+ and activation is widespread. In mice, the quantification of DCX+ cell number/distribution, microglia/macrophage density and infarct volume was performed in three coronal sections at 0.02, 0.5, 0.98 mm rostral from bregma. The DCX+ cell number/distribution was quantified using a 0.0625 mm^2 quadratic grid on an epifluorescence microscope with a 40 x objective. The Iba1+, Iba1+/ED1+, CD16/32+ (M1 marker) microglia/macrophage densities were assessed by first defining the striatal region, and counting positive cells using the Visiopharm software, and then calculating cell density by dividing cell number by striatal area. For infarct volume estimation, images of NeuN-DAB stained sections were first taken under 4 x magnification. Intact areas identified by NeuN+ cells in the ipsilateral and contralateral hemispheres were delineated and then measured using Visiopharm software. The area of unlesioned tissue in the ipsilateral hemisphere was subtracted from that of the contralateral hemisphere to get infarct area, and this area was subsequently multiplied by the distance between the sections (240 μm) to get infarct volume. Mouse and rat cells double-labeled with different markers in epifluorescence microscopy were randomly selected and co-expression validated by confocal microscopy (Carl Zeiss JenaGmbH, Germany) using orthogonal views of single optical sections from confocal Z-series.

For 3D reconstruction of the grafts, area covered by transplanted cells was delineated using human-specific marker SC101 and GFP immunostainings. Coronal sections were assembled using cinema 4D software (Maxon). For quantification of transplanted lt-NES cells, numbers of cells immunoreactive for the different markers were estimated

stereologically using C.A.S.T.-Grid software. Around 500 cells per animal were counted in a pre-defined fraction of the graft area in an epifluorescence/light microscope. Results for NeuN and Ki67 were expressed as percentage of total number of SC101+ cells. For human-specific GFAP and KGA, the fraction of grafted area (GFP+) immunoreactive for each marker was identified with defined representative ranges of threshold for specific signal using image analysis with CellSens Dimension 2010 software (Olympus, Tokyo, Japan), which calculated the total area covered by pixels/specific immunopositive signal. Colocalization of different markers was in all cases validated in a confocal microscope. To estimate fiber density, GFP+/SC121+ immunostaining was used. All fibers crossing the rostral turn of RMS and fibers arriving to the MOB were counted and compared between groups. For analysis of migration, all nuclei of grafted cells were located based on SC101 immunostaining. Distance from each grafted cell to the injection site was calculated using ImageJ software. Mean and maximum distances of migration were compared between groups.

Immuno-electron microscopy

Rats were deeply anesthetized with pentobarbital and transcardially perfused with 0.1M PBS followed by ice-cold 2% PFA, containing 0.2% glutaraladehyde, in 0.1M PBS, pH 7.4. Brains were removed and then washed in 0.1M PBS. Frontal 150 μm sections of whole brain were cut on a Vibratome VT1000A (Leica, Germany). The sections were cryoprotected, freeze-thawed in liquid nitrogen, and incubated overnight in primary goat anti-GFP antibody (1:500, Novus Biologicals) at 4 °C. Tissue was then incubated at room temperature for 2 h with biotinylated rabbit anti-goat secondary antibody (1:200, Dako Cytomation), and avidin-biotin peroxidase complex (ABC) (Vector Laboratories) followed by DAB and 0.015% hydrogen peroxide. Following DAB reaction, sections of the transplanted cortex were processed for electron microscopy. Immunostained sections were post-fixed in 1% osmium tetroxide in 0.1M PBS, dehydrated in a graded series of ethanol and propylene oxide, and flat-embedded in Epon. For identification of GFP/DAB-labeled synaptic contacts, ultrathin sections were cut with a diamond knife and then counterstained with lead citrate and uranyl acetate. Ultrathin sections were

mounted on grids, examined and photographed using a transmission electron microscope JEM- 100CX (JEOL, Japan). Synapses were defined by the presence of at least two to three synaptic vesicles in a presynaptic terminal, a postsynaptic density in postsynaptic structure, and synaptic cleft.

Electrophysiological recordings

For recordings in slices with optogenetic activation, ChR2 was expressed in neurons in ventral thalamic nuclei using stereotaxic injections of adeno-associated virus with the plasmid AAV5-hSyn-hChR2(H134R)-EYFP in isoflurane-anaesthetized rats at the following coordinates: 3 mm caudal from bregma, 3.3 mm lateral from midline, and 5.8 mm ventral from brain surface with tooth bar at -3.3 mm. A volume of 1.5 µl was injected. At least 10 days following virus injection, coronal brain slices were prepared (Oki et al., 2012). Slices were constantly perfused with carbonated artificial CSF (in mM: 119 NaCl, 2.5 KCl, 1.3 $MgSO_4$, 2.5 $CaCl_2$, 26 $NaHCO_3$, 1.25 NaH_2PO_4, and 11 glucose, pH 7.4) at 34°C. Recording pipettes were filled with intracellular solution (in mM: 122.5 potassium gluconate, 12.5 KCl, 10 HEPES, 2.0 MgATP, 0.3 Na_2-GTP, and 8.0 NaCl). Biocytin (1-3 mg/ml) was dissolved in the pipette solution for post hoc identification of recorded cells. Grafted GFP+ cells were identified by autofluorescence, and infrared differential interference contrast microscopy was used when approaching recording pipette to target cell. Whole-cell patch-clamp recordings were performed with EPC10 amplifier using PatchMaster (HEKA) for data acquisition. Cells were held in voltage-clamp at -70 mV. Photo-stimulation was elicited by pulses of blue light (LED-460 nm, Prizmatix) lasting 5 ms applied through a water immersion objective (Olympus, 40 x/0.8) with a maximum power density of 1 mW/mm^2. Data were analysed offline with FitMaster (HEKA), IgorPro and NeuroMatic (Wavemetrics). For *in vivo* electrophysiological recordings and sensory stimulation, rats were anaesthetized and placed in a stereotactic frame. *In vivo* neuronal activity in response to tactile stimulation was recorded by an electrode inserted into the graft or intact brain.

Flow cytometry

Choroid plexus tissue was diced and re-suspended in a 37°C papain, neutral protease (dispase II), DNAse I (PPD) solution and incubated for 30 min at 37°C. The PPD solution was prepared as follows: 2.5 U/ml papain (Worthington Biochemical Corporation), 250 U/ml DNAse I (Worthington Biochemical Corporation), and 1 U/ml dispase II (Roche) were dissolved in DMEM containing 4.5 g/l glucose at 37°C, filter-sterilized and stored at -20°C prior to use. Tissue was then triturated, and excess DMEM/F12 with glutamine (500 µl/50ml) and 10% FBS medium was added. Cells were washed by centrifugation, re-suspended in FACS block buffer (2% FBS in PBS) and strained through a 40 µm strainer. Cells were re-centrifuged and re-suspended in FACS block buffer with CD16/32 antibody (1:100, BD Biosciences) for 10 min at 4°C. Cells were then incubated with antibodies for 30 min at 4°C. Brilliant Violet 421-conjugated rat anti-mouse/human CD11b (1:100, BioLegend) and Brilliant Violet 510-conjugated rat anti-mouse CD45 (1:100, BioLegend) were used. Cells were washed by centrifugation at 4°C and re-suspended in 200 µl FACS buffer (1% BSA in PBS) to be ready for FACS analysis (BD FACS LSRII, Becton Dickinson, Franklin lakes, NJ). Because of the small volume of CSF samples, 20 µl FACS block buffer were first added to CSF. Then the samples were incubated with antibodies as mentioned above. After incubation, 100 µl FACS buffer were added. DRAQ5 (1:200, Thermo Scientific) and 2 µl propidium iodide (PI) were added to the CP and CSF samples before analysis for the identification of live cells.

For microglia sorting from rats or mice, animals were decapitated, brains were rapidly removed and placed in Leibovitz-15 (L-15) media. Brains were then placed in a brain matrix and cut into 1 mm thick coronal sections and the striatum and SVZ were then micro-dissected in L15 media. All solutions and instruments were kept ice-cold until this point. In a laminar hood, tissue was diced and re-suspended in a 37°C papain, neutral protease (dispase II), DNAse I (PPD) solution and incubated for 30 min at 37°C. Tissue was then triturated, and excess DMEM/F12 with glutamine (500 µl/50 ml) and 10% FBS medium was added. Cells were washed by centrifugation, re-suspended in medium and strained through a 40 µm strainer. Cells were then re-centrifuged and re-suspended in 4 ml 37% percoll. 4 ml 70% percoll was slowly underlaid and 30% percoll added on top followed by an additional 2 ml of media. A gradient was then run for 40 min, 200x g at

18°C. Minimal acceleration and brake settings were used. The thick viscous layer of debris formed was removed and the halo-like ring of brain-microglia formed between the 70% and 37% gradients was collected and washed by centrifugation in media. Cells were then re-suspended in FACS block buffer (0.1% FBS in PBS) with antibodies for 30 min at 4°C. For rat microglia sorting, Allophycocyanin (APC)-conjugated mouse anti-rat CD11b (1:100; Life Technologies) and R-Phycoerythrin (RPE)-conjugated mouse anti-rat CD45 (1:10; AbDSerotec) antibodies were used. For mouse microglia sorting, Brilliant Violet 421-conjugated rat anti-mouse/human CD11b (1:200, BioLegend) and Brilliant Violet 510-conjugated rat anti-mouse CD45 (1:20, BioLegend) antibodies were used. Cells were then washed by centrifugation at 4 °C and re-suspended in 400 µl FACS buffer (1% BSA in PBS) to be ready for FACS sorting (BD FACSAria™ III, Becton Dickinson, Franklin lakes, NJ). 2 min prior to sorting, 2 µl PI was added to the sample for the identification of dead cells. A minimum of 50 000 and 10 000 cells were collected for striatum and SVZ samples, respectively. Cells were directly sorted into RLT buffer (Qiagen) containing 1% beta-Mercaptoethanol and were immediately frozen on powdered dry ice.

RNA extraction and quantitative PCR

Total RNA was extracted from cells or tissue using a RNeasy Plus micro kit (Qiagen), and then reversed to cDNA using a qScript cDNA Synthesis Kit (Quanta Bio). For quantitative PCR, TaqMan Gene expression master mix (Life Technologies) and TaqMan probe were used. Cycle threshold values of target genes were normalized to geometric mean of housekeeping HPRT and GAPDH to get ΔCt. 2 to the power of -ΔCt were calculated for final analysis. The DNA band was examined after running in a 2% agarose gel at 90 mV for 1 h. The following Taqman probes were used for qPCR analysis:

Gene Name	**Gene Function**	**Taqman probe Number**
Hprt	Housekeeping gene	Mm03024075_m1
Gapdh	Housekeeping gene	Mm99999915_g1

Nt5e	Leukocyte transmigration mediator	Mm00501910_m1
Ifnγ	Choroid plexus activator	Mm01168134_m1
Mcp1	Chemokine	Mm00441242_m1
Cx_3cl1	Chemokine	Mm00436454_m1
Madcam1	Adhesion molecule	Mm00522088_m1
Vcam1	Adhesion molecule	Mm01320970_m1
Tnfα	M1-like macrophage marker	Mm00443258_m1
Igf1	M2-like macrophage marker	Mm00439560_m1
Ym1	M2-like macrophage marker	Mm00657889_mH
Tgfβ1	M2-like macrophage marker	Mm01178820_m1
Arg1	M2-like macrophage marker	Mm00475988_m1

GeneChip microarray assay

Sample preparation for microarray hybridization was carried out as described in the NuGEN Ovation Pico WTA System V2 and Encore Biotin Module manuals (NuGEN Technologies, Inc, San Carlos, CA). In brief, 2 to 10 ng of total RNA was reverse transcribed into double-stranded cDNA in a two-step process, introducing a SPIA tag sequence. Good quality of RNA and cDNA was confirmed by the company performing microarray analysis (KFB—Center of Excellence for Fluorescent Bioanalytics, Regensburg, Germany; www.kfb-regensburg.de). Bead-purified cDNA was amplified by a SPIA amplification reaction followed by an additional bead purification. 3.0 µg of SPIA cDNA were fragmented, terminally biotin-labeled and hybridized to an Affymetrix Rat Gene 1.1 ST Array Plate. For hybridization, washing, staining and scanning, an Affymetrix GeneTitan® system was used (Affymetrix, Inc., Santa Clara, CA). Sample processing was performed at an Affymetrix Service Provider and Core Facility, "KFB—Center of Excellence for Fluorescent Bioanalytics".

Global gene expression microarray analysis

Summarized probe set signals were calculated by the RMA algorithm with the Affymetrix GeneChip Expression Console Software. Average signal values, comparison fold changes and significance p values were calculated using affy and limma package in R software by comparing SVZ/Striatum samples of LPS or MCAO groups with that of naïve groups. Only genes with changes greater than 1.5 fold and with an adjusted p value < 0.05 were identified. Genes coding secreted proteins were identified by GO: 0005576. Common upregulated or downregulated genes in SVZ and striatum of LPS and MCAO groups were identified using VENNY software (http://bioinfogp.cnb.csic.es/tools/venny/index.html). Among genes that were significantly changed in striatal microglia sorted from MCAO or LPS condition compared with naïve one, we identified factors that differed significantly between MCAO and LPS conditions ($p < 0.05$) and for which the fold difference was > 1.5.

Cell culture

For SVZ explant culture, mouse pups were decapitated at postnatal days 4-5 (P4-P5), brains were removed, placed in ice-cold L-15 medium and cut into 250 µm sections on a vibratome. Sections containing SVZ were collected and the SVZ were dissected from the lateral wall of the anterior horn of the lateral ventricle and cut into small explants (approx. 100-200 µm in diameter). These were then mixed with Matrigel (Corning) and cultured in four-well dishes. After polymerization (25 min), 500 µl of Neurobasal medium supplemented with B-27, N2-supplement, glutamine, and penicillin/streptomycin (all from Gibco-Life Technologies) were added. Cultures were maintained in a humidified, 5% CO_2, 37 °C incubator with mouse CXCL13 (2, 5, 10, or 20 µg/mL; R&D Systems) or CXCL12 (50 ng/ml; R&D Systems). The length of migratory chains was measured from the edge of the explants at three angles using Image J software (NIH, Bethesda, MD, USA) after 24 h.

For M2-like macrophage generation, monocytes were isolated as mentioned above and then cultured at 0.5 x 10^6cells/ml in RPMI-1640 medium supplemented with 10% FBS, 1mM L-glutamine, 1mM sodium pyruvate, 100 U/ml penicillin, 100 mg/ml streptomycin, 50 ng/ml M-CSF (Peprotech), 50 ng/ml IL4 (Peprotech) and 25 ng/ml IL13 (Peprotech). Five days later, macrophages were collected, washed and resuspended in PBS for transplantation.

For iPSC generation, human fibroblasts were subjected to retroviral transduction with plasmids encoding for the viral glycoprotein VSV-G and the reprogramming factors (Oct4, Sox2, KLF4 and c-MYC) and split into plates with mouse embryonic fibroblasts. Colonies were then picked and expanded to establish human iPSC lines. Those lines were induced to differentiate to neural phenotype as previously described through an embryoid body-production step (Koch et al., 2009). Neural rosettes were generated and carefully picked and grown in the presence of 10 ng/ml FGF2, 10 ng/ml EGF (both from R&D systems) and 1 µl/ml B27 (Invitrogen). The human iPSC-derived lt-NES cells line is routinely cultured and expanded on 0.1 mg/ml poly-L-ornithine and 10 mg/ml laminin (both from Sigma) coated plates into the same media supplemented with FGF, EGF and B27. The human iPSC-derived lt-NES cells were passaged at a ratio of 1:2 to 1:3 every second to third day using trypsin (Sigma). The lt-NES cells were primed towards a cortical neuronal phenotype (Tornero et al., 2013). Briefly, growth factors (FGF, EGF) and B27 were omitted and cells were cultured at low density in differentiation-defined medium in the presence of BMP4 (10 ng/ml), Wnt3A (10 ng/ml) and cyclopamine (1mM) for 7 days. Neuronal progenitors were then dissociated using trypsin and prepared for transplantation.

Lentivirus production and transduction

The construct for the tracing vector was purchased from AddGene (ID: 30195). High-titter preparations of lentiviral particles were produced according to protocol from Dull et al. in a biosafety level 2 environment (Dull et al., 1998). The lt-NES cells were stably transduced with 10% of lentiviral tracing vector during 48 h and checked 1 week later under inverted fluorescence microscope (Olympus) for nuclear GFP expression. The

efficiency of transduction was about 80%.

ΔG-Rabies vector production and injection

Pseudo-typed rabies vector was produced as previously described with minor adjustments (Osakada and Callaway, 2013). The protocol was stopped after step 60 as the virus was concentrated via ultracentrifugation only once and no sucrose cushion was used. Tittering was performed using TVA-expressing HEK 293 T cells as defined in the protocol. Titters were 20-30 x 10^6 TU/ml. For *in vivo* experiments, we used a dilution of 5%, as determined by testing different dilutions for a concentration that gave specific infection and tracing, in the absence of toxicity. At 2 or 6 months after cell transplantation, intracortical ΔG-rabies vector injection was performed stereotaxically at the following coordinates (coordinates 1: 0.5 mm rostral from bregma, 2.5 mm lateral from midline, 2.5 and 1mm ventral from brain surface. coordinates 2: 0.7 mm rostral from bregma, 2.95 mm lateral from midline, 2.5 and 1.5 mm ventral from brain surface. coordinates 3: 0.4 mm rostral from bregma, 2.7 mm lateral from midline, 2.5 and 1.5 mm ventral from brain surface; tooth bar at -3.3 mm). A volume of 1 µl was injected at three sites with two deposits in each (6 µl of 5% ΔG-rabies vector in total). For control experiments, intact rats were injected in the same way with lentiviral tracing vector and 1 week later with ΔG-rabies vector. Animals were sacrificed 1 week later.

Behavioral tests

All behavioral tests were performed by investigator blinded to treatment conditions.

For open field test, mice were brought into the test room 30 min before the test to acclimate the mice to the environment. During the whole 1 h test, the test room was kept in darkness. For the test, mice were kept in a black box equipped with a camera. Movements of the mice were automatically recorded using ANY-MAZE software (Stoelting Co., UK). Various parameters of mice movement, such as total movement distance, time spent on movement (Time immobile), mobile episode number, clockwise rotation number, anti-clockwise rotation number, time freezing, rearing number and

central zone entries number were obtained automatically by the software. Twelve sessions of individual 5 min test were acquired and averaged for further analysis.

The corridor test adapted to mice was used to assess sensorimotor impairment (Dowd et al., 2005; Grealish et al., 2010). Briefly, animals were food-deprived 12 h before the first testing day and kept on a restricted food intake (2.5-3.5 g/d) so that the body weight did not fall below 85% of initial value. Food was provided only after the daily test session. At the first time point, mice were habituated to the corridor by scattering sugar pellets along the floor and allowing them to freely explore for 10 min on 2 consecutive days before testing. When testing began, the mice were transferred to one end of the testing corridor. The numbers of ipsilateral and contralateral retrievals were counted until a maximum time of 5 min had elapsed. A "retrieval" was defined as an exploration into a pot, whether or not a pellet was eaten, and a new retrieval could only be made by investigating a new pot. Two sessions of the test were done for each mouse in one test day. Retrieval average was calculated for the total 5 testing days. Contralateral side touches (% of total) were expressed as percentage of pellets eaten or smelled on the contralateral side out of those on contralateral and ipsilateral sides combined.

The cognitive function of mouse was assessed based on their escape behavior (Sansone et al., 1993) in an automated step-through type system (GEMINI, San Diego Instruments Inc., San Diego, CA, USA). The equipment software controls the opening of the gate between the two boxes and the electrical shocks on grid floor. On the first day (pre-training day), the tested mouse was allowed to habituate to the environment with both boxes in darkness and gate opened for 10 min. For active avoidance test training, the light turned on in the box opposite to where the mouse was. When the mouse stayed in the dark box over 30 s, it received an electrical shock of 1 mA for 5 s. This was repeated 30 times during the first training day and the number of moving to the illuminated box was counted as the number of avoidances. This training was performed in all mice for a total of three days in the same way. Five days after last day of training, mice were tested in the same way as in the training but without any electric shock and the number of avoidances was counted. This trial test was repeated for 4 days.

Statistical analysis

Comparisons were performed using Prism 6 software (GraphPad Software, Inc.) by one-

or two-way ANOVA followed by Bonferroni's post hoc test, or Student's unpaired t test. To achieve normal distribution of data, counts of DCX+ cells in stroke and LPS-treated groups values were subjected to log10 transformation and parametric statistical analysis was then performed. Data are presented as means ± SEM, and differences are considered significant at $p < 0.05$.

Results

Inflammation without neuronal loss triggers striatal neurogenesis (Paper I)

Establishment of a striatal inflammatory model without neuronal loss

For this purpose, we injected 15 μg LPS into rat striatum. Two weeks later, there was extensive inflammatory response in the striatum, as characterized by 2-fold increase in Iba1+ microglia/macrophage numbers as compared with vehicle injection group. This inflammatory response was comparable to that after striatal stroke. At 6 weeks after LPS injection, the inflammatory response had subsided to baseline level. In contrast to the extensive neuronal loss in the striatum caused by MCAO, we did not detect any obvious neuronal injury in the LPS-injected striatum.

Neurogenesis in inflammatory striatum without neuronal loss

We then quantified striatal neurogenesis in the LPS-induced inflammation model. Two weeks after injection, we found a large number of DCX+ neuroblasts in the striatum, comparable to that after ischemic stroke. The increased number of DCX+ neuroblasts in the striatum remained at 6 weeks after LPS injection. At 6 weeks, we also found increased number of NeuN+/BrdU+ new mature neurons in the LPS-injected striatum similar to what was observed after stroke. These data suggest that neurogenesis is triggered by inflammation in the striatum also in the absence of neuronal loss. The level of neurogenesis is comparable to that after ischemic stroke.

Microarray analysis of microglia sorted from stroke-affected, LPS-injected and naïve rats

We sorted out microglia from SVZ and striatum of three groups of rats: rats subjected to stroke, injected with LPS and without any treatment, respectively, at 2 weeks time-point.

We then extracted RNA from the sorted microglia, reversely transcribed RNA to cDNA, and performed a microarray analysis of the obtained cDNA. We identified several genes coding extracellular proteins that were significantly upregulated more than 1.5-fold in both SVZ and striatum samples, in both stroke-subjected and LPS-injected rats as compared to naïve ones. Potentially, these proteins could be involved in regulating different steps of neurogenesis. We selected Cxcl13 which we hypothesized could contribute to the regulation of striatal neuroblasts migration and further examined its role.

Role of Cxcl13 for neuroblasts migration in vitro and in vivo

We first confirmed that Cxcl13 was expressed in mouse microglia using PCR. We then cultured mouse SVZ explants *in vitro* and added different doses of CXCL13 protein to the culture system. At doses higher than 5 µg/ml, CXCL13 promoted neuroblasts migration. However, this effect was weaker than that observed after addition of CXCL12. At variance with the *in vitro* results, neuroblasts migration after stroke in mice lacking the Cxcl13 receptor ($Cxcr5^{-/-}$mice) did not differ from that in wild-type control mice. We examined the ischemic damage in $Cxcr5^{-/-}$ mice and found that these mice had bigger stroke-induced lesion volume than control animals. Also, we found that the inflammatory response was more intense in $Cxcr5^{-/-}$ mice compared with control, as characterized by increased density of CD16/32+ pro-inflammatory microglia/macrophages. Taken together, these data indicate that the Cxcl13/Cxcr5 pathway promotes neuroblasts migration *in vitro* and has a neuroprotective effect *in vivo*.

Choroid plexus activation and enhancement of M2-like MDM infiltration via CSF route after stroke (Paper II)

Response of CP to cortical stroke

We first examined whether CP is activated after cortical stroke. For this purpose, several factors were analyzed which had previously been shown to be upregulated in CP after spinal cord injury, and could mediate MDM migration via CP (Shechter et al., 2013). We

found that Nt5e was upregulated in ipsilateral CP at 6 h after stroke. At 24 h after stroke, Vcam1, Madcam1 and Cx_3cl1 showed upregulation in CP and Cx_3cl1 remained upregulated also at 3 days after stroke. At 7 days, Nt5e showed upregulation but at 14 days, both Cx_3cl1 and Nt5e were downregulated. Taken together, these data provide evidence that CP responds to cortical ischemia by upregulating several potential MDM migration mediators, and that this response occurs mainly within the first 3 days after stroke.

Increased MDM infiltration in CP and CSF after stroke

We then assessed whether there were changes of MDM infiltration in CP and CSF after stroke. Consistent with the upregulation of the potential MDM migration mediators in CP at 24 h and 3 d after stroke, we found that the density of CD45+/CD11b+ MDM increased in CSF at 24 h, and returned to baseline level at 3 days after stroke. In CP, the amount of CD45+/ CD11b+ MDM, as evidenced by the percentage of CD45+/CD11b+ MDM out of total live cells, increased at 3 days but was unaltered at 24 h after stroke. These data suggest that CP might mediate MDM infiltration into CSF after stroke.

Infiltration of MDM from CSF into injured area of the brain

We wanted to know whether the increased number of MDM found in CSF was followed by migration of these cells into ischemic hemisphere after stroke. We isolated CD115+ monocytes from bone marrow of Cx_3cr1^{GFP}mice using magnetic-activated cell sorting (MACS). We then injected the freshly isolated Cx_3cr1^{GFP} monocytes into ipsilateral lateral ventricle at 24 h after stroke. Three days later, we found a large number of GFP+ MDM in the area surrounding the lesion site. Some of the infiltrated cells showed round morphology, indicating that they had been activated. We also injected Cx_3cr1^{GFP} monocytes into the contralateral ventricle at 24 h after stroke and examined the brains 3 days later. Again, we found large numbers of GFP+ MDM in the area around the lesion site. Taken together, these data indicate that MDM in CSF migrate into the ischemic hemisphere after stroke.

Enhancement of infiltration of anti-inflammatory M2-like MDM via CSF route promotes recovery after stroke

We explored whether we could take advantage of our finding that MDM can migrate through CSF to the stroke-injured site in order to enhance the infiltration of anti-inflammatory M2-like MDM. To test this idea, we isolated CD115+ monocytes and cultured them with IL4 and IL13 for 5 days. Using qPCR, we found that after IL4 and IL13 treatment, many M2 markers were upregulated, indicating that they had been primed to M2-like macrophages. We then wanted to know whether the *in vitro*-derived M2-like MDM could migrate into the ischemic hemisphere after delivery into CSF. We injected the M2-like Cx_3cr1^{GFP} MDM into the ipsilateral lateral ventricle at 24 h after stroke. 3 days later, we found a large number of GFP+ MDM in the area around the ischemic lesion. At this time point, infiltrated cells expressed the M2-like MDM markers CD206 and YM1.

We then established two groups of mice, which were subjected to stroke and then received either M2-like MDM or vehicle into the lateral ventricle. We examined some mice at 7 days after transplantation and found that the two groups had similar infarct volume. At 3 weeks, mice injected with M2-like MDM showed improved motor performance, as evidenced by increased anti-clockwise rotation in open field test and increased preference of smelling or eating pellet on the contralateral side in corridor test. These differences disappeared at 3 months after transplantation. Both at 3 weeks and 3 months after transplantation, mice injected with M2-like MDM exhibited increased travel distance in the open field test. These findings indicate that M2-like MDM, delivered into CSF of stroke-subjected mice, migrate into ischemic hemisphere, maintain their M2-like phenotype, and give rise to both transient and stable improvements in the recovery of stroke-impaired motor functions.

We also examined the effect of M2-like MDM on cognitive performance using active avoidance test. While mice injected with M2-like MDM showed no difference as compared to vehicle-injected animals in learning curve at 2 weeks after stroke, they exhibited significantly better performance at 3 months after transplantation. The

improved functional recovery elicited by M2-like MDM was not due to reduced ischemic damage because infarct volume was similar in cell- and vehicle-injected groups. We then asked whether the M2-like phenotype of MDM is essential for the motor and cognitive improvement. Therefore, we transplanted freshly isolated monocytes in the same way as with the M2-like MDM. However, at 3 weeks after transplantation of freshly isolated monocytes, we did not observed any improvements in either corridor and open field tests or active avoidance test. Our findings demonstrate a beneficial role of M2-like MDM, infiltrating the stroke-injured brain through the CSF route, in promoting post-stroke recovery.

Effect of stroke on behavior of human iPSC-derived lt-NES cells transplanted adjacent to a neurogenic area (Paper III)

Survival, proliferation and differentiation of human iPSC-derived lt-NES cells after transplantation into stroke-injured brain

We transplanted human iPSC-derived lt-NES cells into the rostral migratory stream (RMS), adjacent to the neurogenic SVZ, of intact rats and rats subjected to striatal stroke 48 h earlier. We first compared the survival of the transplanted cells between intact and stroke-affected animals at 2 months after transplantation using human cell-specific SC101 as a marker, and found no difference between the groups. The percentage of Ki67+ proliferating cells and DCX+ neuroblasts within the grafts was also similar. Moreover, the two groups exhibited no difference in the percentage of either NeuN+ mature neurons or GFAP+ astrocytes in the grafts. Taken together, these data indicate that the ischemic lesion did not influence the survival, proliferation or neuronal/astrocytic differentiation of the transplanted human iPSC-derived lt-NES cells.

Migration and axonal projection patterns of transplanted human iPSC-derived lt-NES cells

We then examined the migration pattern of the human iPSC-derived lt-NES cells after

transplantation adjacent to the SVZ. In intact rats, the transplanted cells migrated along the descending limb of the RMS, but never reaching beyond the rostral turn of RMS. In rats subjected to stroke, the grafted cells showed a completely different migration pattern. In this case, the transplanted cells migrated in the opposite direction towards the ischemic striatum. The average distance of migration was longer for cells implanted in stroke-affected rats as compared to that in intact rats. We finally analyzed the axonal projection pattern of the transplanted cells. In intact rats, the human iPSC-derived lt-NES cells sent a large number of fibers along RMS, reaching the granular and glomerular layers of the main olfactory bulb (MOB). In contrast, in the stroke-injured animals, virtually no fibers reached the granular layer of the MOB and only very few the rostral turn of the RMS. Taken together, these data show that a stroke-induced lesion alters the migration and axonal projection patterns of transplanted human iPSC-derived lt-NES cells.

Synaptic input from stroke-injured host brain to grafted neurons generated from human iPSC-derived lt-NES cells (Paper IV)

Formation of afferent synapses on transplanted cortical neurons

We transplanted GFP+ cortical progenitors differentiated from human iPSC-derived lt-NES cells into an area adjacent to the somatosensory cortex at 48 h after dMCAO. Six months later, the rats were sacrificed and examined for synapse formation using immunoelectron microscopy. We found that GFP- host axon terminals formed ultrastructurally authentic synaptic contacts on most of the GFP + grafted neurons. The majority of the afferent synaptic contacts were axo-dendritic and only 8.4% were axo-somatic. All axo-dendritic contacts were asymmetric with structural characteristics of excitatory/glutamatergic synapses, 84.7% of which were in contact with GFP + dendritic spines. The host axon terminals displayed abundant synaptic vesicles, and particularly docked vesicles at the presynaptic membrane. Taken together, these data indicate that neurons derived from transplanted human iPSC-derived lt-NES cells receive synaptic inputs from host neurons that resemble ultrastructurally functional synapses in the host brain.

Brain areas of origin of afferent synaptic inputs on the grafted neurons

We transfected the cortical progenitors derived from human iPSC-derived lt-NES cells with tracing vectors and then transplanted the cells intracortically at 48 h after dMCAO. Two months later, we injected ΔG-rabies virus vector into the location of the grafted cells. Using this rabies virus trans-synaptic tracing technique, we were able to identify host neurons that form direct synapses on the grafted neurons. We found high density of traced neurons in the cortical area adjacent to the graft, in the area corresponding to the location of the graft in contralateral cortex, and bilaterally in dorsal claustrum. Most importantly, a large number of traced neurons were found in the thalamus, which mediates sensory information from the periphery to the somatosensory cortex. The highest density of traced neurons was located in ventral and posterior nuclei whereas no traced neurons were found in anterior nuclei or reticular nucleus. When ΔG-rabies vectors were injected into the same location as the graft but in the intact rat brain, the traced neurons showed the same distribution pattern in different areas. Taken together, our data show that grafted cortical neurons, generated from human iPSC-derived lt-NES cells, receive axonal projections from various brain areas in the host and that the projection pattern closely resembles that in the intact brain.

Response of grafted neurons to physiological sensory stimuli

To examine the function of the synapses from the host on the transplanted neurons, we recorded their electrophysiological activity in anaesthetized rats while performing tactile stimulation of different body areas at 3 months after transplantation. We used the following criteria to identify signals from the grafted neurons:(1) recordings from the center of the grafts with over 70 μm distance to the border of the graft, defined by post-mortem 3D immunohistochemistry; (2) spike amplitude of >100 μV and signal to noise ratio of over 2.5. We identified 10 recordings in the grafts fulfilling these criteria. All but one of these neurons received a short latency (within the first 50 ms from stimulation onset) excitatory input from the nose with onset latency ranging from 9 to 32 ms. Four

neurons received an additional short latency excitatory input from either the ipsilateral forepaw, the contralateral forepaw, the ipsilateral hindpaw or the contralateral hindpaw. Spontaneous activity in four neurons was inhibited by tactile stimulation of at least one body area with an onset latency of between 46 and 85 ms. These data suggest that at least some of the synapses formed on the transplanted neurons by host neurons are functional *in vivo*.

Response of grafted neurons to optogenetic activation of thalamic afferent axons

To confirm the functionality of the synaptic inputs, we used optogenetics to investigate the response of the transplanted neurons to activation of thalamic afferent axons. Rats subjected to dMCAO were transplantated with lt-NES cells 48 h later and ventral thalamic nuclei sending axons to somatosensory cortex were labeled with photo-responsive ChR2 at 2 months after transplantation. After 10-34 days, we performed patch-clamp recordings from grafted GFP + cells while photo-stimulating thalamic pre-terminal axons in acute brain slices. Of nine recorded cells with neuronal electrophysiological characteristics, two cells responded to light stimulation. During depolarizing current injections, one cell exhibited regular spiking pattern, typical of pyramidal neurons, while the other exhibited fast-spiking behavior, typical of a subset of GABAergic interneurons. Notably, the neurons in ventral thalamic nuclei labeled with ChR2 showed morphology and distribution similar to what we had observed with the monosynaptically traced cells that project to the graft or corresponding cortical area in the rabies virus experiment. Taken together, these findings show that the synapses formed on transplanted neurons by host thalamic neurons are functional.

Discussion

In this thesis, we report four main findings: First, inflammation without neuronal loss is sufficient to trigger neurogenesis in rat striatum, which is comparable to that after stroke. Several microglia-derived factors, e.g., Cxcl13, were identified which could regulate different steps of striatal neurogenesis. Second, CP acts as a pathway for MDM infiltration into the brain after stroke. The M2-like MDM taking this route might play important roles in promoting both motor and cognitive recovery. The infiltration could be enhanced by M2-like MDM delivery into CSF. Third, a stroke-induced lesion influences the migration and axonal projection patterns of transplanted iPSC-derived lt-NES cells but has no effect on their survival, proliferation or differentiation. Fourth, as evidenced by electron microscopy, rabies virus trans-synaptic tracing, *in vivo* electrophysiological recording and optogenetic techniques, neurons differentiated from transplanted iPSC-derived lt-NES cells receive functional synaptic inputs from the correct host brain areas and respond to tactile stimulation in the stroke model.

Inflammation and stroke recovery

In rodents, neurogenesis occurs in the striatum after stroke and the number of neuroblasts recruited to the striatum correlates positively with the size of infarct volume (Arvidsson et al., 2002; Thored et al., 2006). Whether it is the neuronal death after stroke or the accompanying inflammation that triggers striatal neurogenesis has been unknown. Using a rat model, in which LPS injection induces inflammation without neuronal loss, we found that neurogenesis still occurs in the striatum at a level comparable to that after stroke. In sorted microglia from rats subjected to stroke and LPS injection, we identified several upregulated factors that have previously been reported to regulate neurogenesis *in vitro* or *in vivo*. FGF2 has been shown to maintain a slow-dividing NSPC pool in adult mouse SVZ (Zheng et al., 2004), and TNFSF12 was found to inhibit adult mouse SVZ NSPC proliferation and promote neuronal differentiation (Scholzke et al., 2011). Deficiency of another factor, Complement 3 (C3), decreased ischemia-induced neurogenesis in SVZ (Rahpeymai et al., 2006). Our data suggest that the inflammation

associated with stroke is the main inducer of striatal neurogenesis, and that microglia play an important role in this process.

Besides brain resident microglia, blood-borne macrophages are important inflammatory cells in CNS pathology. We previously showed that blood-borne macrophages infiltrate the ischemic hemisphere and contribute to post-stroke motor recovery (Wattananit et al., 2016). This effect might be attributed to M2-like macrophages and their derived factors (Liu et al., 2016b; Wattananit et al., 2016). Seemingly in contrast to these findings, intravenous administration of M2-like macrophages had no effect on motor recovery up to 2 weeks after stroke in rats (Desestret et al., 2013). Here, we have provided direct evidence that M2-like macrophages promote both motor and cognitive recovery after stroke. This effect is not due to reduced ischemic damage, but possibly by enhancement of axonal growth or plasticity in existing neuronal circuits.

We have also provided evidence that MDM, including M2-like ones, can take the CP-CSF route for infiltration after stroke, echoing the findings in spinal cord injury (Shechter et al., 2013). Our findings raise the possibility that enhancing M2-like MDM infiltration via CP by anti-PD1 antibody (Baruch et al., 2016), or application of compounds that can skew macrophages towards M2-like fate (Feng et al., 2016), might lead to improved post-stroke recovery. Moreover, it might be possible to transplant M2-like MDM, derived from the stroke patients' own blood, into CSF for promoting motor and cognitive recovery. Interestingly, intrathecal injection of macrophages with M2-like phenotype derived *in vitro* has in preliminary experiments been reported to improve neurological performance in stroke patients without any significant adverse effects (Chernykh et al., 2016).

Transplantation of human iPSC-derived lt-NES cells for promoting stroke recovery

A fundamental question in the field of transplanting NSPC and their derivatives to treat stroke is whether the generated neurons could become functionally integrated into host neuronal circuitry. We have previously observed that cortical neurons, generated from human iPSC-derived lt-NES cells, send efferent projections to cortical and subcortical

areas, and that host neurons might form afferent synapses on the grafted neurons (Tornero et al., 2013). Similarly, host neurons were found to form synaptic contacts on murine NSPC-derived neurons after transplanted into a rat model of striatal lacunar infarction (Muneton-Gomez et al., 2012). Using immunoelectron microscopy, we have provided evidence that cortical neurons generated from human iPSC-derived lt-NES cells receive synaptic inputs from host neurons after intracortical transplantation in rats subjected to cortical stroke. Using the rabies virus tracing technique, we found that the projecting axons originated in cortical areas adjacent to the graft, contralateral cortex corresponding to the location of the graft, bilateral dorsal claustrum, as well as the ventral and posterior nuclei of the thalamus. The distribution pattern of the areas of origin in the stroke-injured rats closely resembled that in intact rats, indicating that the grafted neurons received afferent inputs from the appropriate host neurons. Similar to our findings, neurons of visual cortex identity derived from murine embryonic stem cells have been shown to receive the correct input from the host brain after transplantation into mice with visual cortex lesion. Neuron identity match between the graft and the host transplantation site was found crucial for efficient integration into the host neural circuitry (Michelsen et al., 2015), which suggests that our fated cortical neurons match well with the sensorimotor cortex neurons lost after stroke.

We finally examined the functionality of the synapses from the host onto the grafted neurons. Grafted neurons responded electrophysiologically to tactile stimuli on the nose and paws in stroke-injured rats with onset latencies of evoked responses similar to those in intact rats. Moreover, optogenetic activation of thalamo-cortical neurons expressing ChR2 was found to elicit electrophysiological responses in the grafted neurons in acute brain slices. These neurons were morphologically similar to the neurons labeled using rabies virus trans-synaptic labeling technique in the thalamus. Our findings strongly indicate that the grafted neurons are functionally integrated into host neuronal circuitry with the appropriate afferent input. Possibly, neuronal integration may also contribute to the improved post-stroke motor recovery at 8 weeks after human iPSC-derived lt-NES cell transplantation (Tornero et al., 2013). Because the level of innervations and maturity of synaptic contacts between the transplanted human neurons and the host increase significantly between 2 and 6 months after transplantation (Avaliani et al., 2014; Espuny-

Camacho et al., 2013), neuronal integration is likely to play a more significant role in long-term post-stroke recovery, while mechanisms such as trophic support mediate mainly short-term recovery (Kokaia et al., 2012).

Interplay between inflammation and transplanted stem cells after stroke

Our findings indicate that inflammation triggers post-stroke neurogenesis and that microglia-derived factors regulate different steps of neurogenesis, which suggests that the inflammation accompanying ischemic stroke might also influence the behavior of transplanted NSPC. To test this hypothesis, we transplanted human iPSC-derived lt-NES cells into RMS of intact rats and rats subjected to stroke. At 2 months after transplantation into intact rats, the grafted cells migrated along RMS, possibly influenced by the same molecular pathways as the ones regulating migration of endogenous neuroblasts. In contrast, after transplantation into stroke-injured rats, the grafted cells migrated towards the ischemic area. Previously, it has been shown that after stroke, neuroblasts generated in SVZ migrate into ischemic striatum (Arvidsson et al., 2002), and microglia-derived chemokines such as CXCL12 and MCP1 are involved in mediating this process (Robin et al., 2006; Thored et al., 2006; Yan et al., 2007). In this thesis, we have also found that microglia-derived CXCL13 promotes neuroblasts migration *in vitro*. Hypothetically, transplanted human iPSC-derived lt-NES cells respond to these and other chemokines released from the inflammatory cells in the ischemic area and migrate towards them.

During development, microglial cells are essential for axonal growth (Mosser et al., 2017), and integration of newborn neurons in adult brain is influenced by activated microglia (Jakubs et al., 2008). Microglia-derived IL-1β has been found to suppress axonal development (Han et al., 2017). These findings suggest that the lack of axonal outgrowth from transplanted human iPSC-derived lt-NES cells along RMS in stroke-injured rats might be caused, at least partly, by factors released from activated microglia. In line with our findings, neuronal differentiation of transplanted spinal cord-derived NSPC is altered by chronic inflammation in experimental autoimmune encephalomyelitis (EAE) model (Covacu et al., 2014).

It has been observed that NSPC transplanted into the diseased CNS can also influence inflammatory responses in the host. Transplanted NSPC attenuate brain inflammation in mouse EAE model (Einstein et al., 2006). Immunomodulation might also, at least partly, underlie the recovery at 8 weeks after human iPSC-derived lt-NES cell transplantation in stroke (Tornero et al., 2013). The immunomodulatory effect of NSPC is mediated by direct contact with phagocytes, influencing the expression of their inflammatory genes (Cusimano et al., 2012), and by certain secreted factors (Cheng et al., 2017). SVZ NSPC can secrete IL15 to sustain functional competence of NK cells (Liu et al., 2016a). NSPC were also found to regulate complement activation via complement receptor type 1-related protein y (Crry) (Gao et al., 2017). Interestingly, NSPC have been reported to skew pro-inflammatory M1-like microglia/macrophages towards anti-inflammatory M2-like phenotype (Cusimano et al., 2012; Gao et al., 2016). The interplay between inflammatory cells and NSPC raises the possibility that modulation of inflammation and NSPC transplantation could be combined to get synergistic effect in promoting recovery in the diseased CNS. Indeed, vaccination of mice with myelin-derived peptide, together with NSPC transplantation, synergistically promoted recovery after spinal cord injury (Ziv et al., 2006). Co-transplantation of NSPC with M2-like macrophages lead to increased neuronal differentiation of engrafted NSPC (Zhang et al., 2015). These observations, together with our findings that both transplantation of human iPSC-derived lt-NES cells and delivery of M2-like MDM into CSF promote post-stroke functional restoration, suggest that combining these two approaches might result in optimum motor and cognitive recovery after stroke.

Concluding remarks

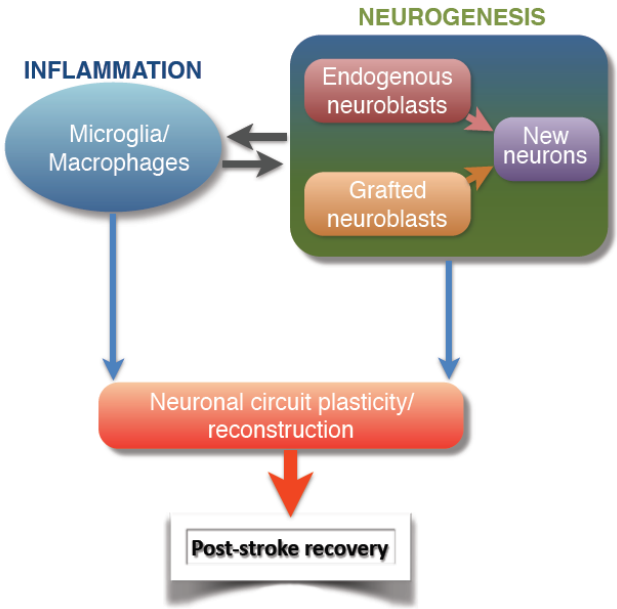

In this thesis, we have obtained evidence that inflammation is a major inducer of striatal neurogenesis after stroke. Our findings also indicate that the CP-CSF pathway might serve as a route for brain infiltration of inflammatory MDM, and that M2-like MDM taking this route play an important role in the recovery of motor and cognitive function after ischemic stroke. Manipulating the inflammatory response and infiltration of M2-like MDM via CP with small or macro- molecules, such as anti-PD1 antibodies (Baruch et al., 2016), might be developed into new therapeutics for promoting post-stroke recovery. Our data also raise the possibility of transplanting M2-like MDM derived from the stroke patients' own blood monocytes into CSF as a new approach to promote post-stroke recovery.

Transplantation of human iPSC-derived lt-NES cells has been shown to promote motor function recovery in rat stroke model (Tornero et al., 2013). We found here that ischemic stroke can influence the migration and axonal projection pattern of transplanted human iPSC-derived lt-NES cells. Therefore, manipulation of post-stroke response such as inflammatory response, should be taken into consideration in order to optimize the therapeutic effect when, in a hypothetical future clinical setting, human iPSC-derived lt-NES cells and their derivatives are transplanted into ischemic patients for promoting recovery. Our evidence that grafted neurons generated from human iPSC-derived lt-NES cells receive the correct functional input from host neurons supports the feasibility of using stem cell-derived neurons to replace the neurons lost after ischemic stroke, thereby promoting recovery.

Acknowledgements

I would like to first thank my supervisor Zaal Kokaia and my co-supervisor Olle Lindvall. During my six years as PhD student, they taught me a lot about how to raise scientific questions, how to design experiments to answer these questions, how to set go-no-go points, and how to finally write a good "story" based on our findings. They are the epitomes of the spirit of "Never give up!", and working with them in these years also instills the spirit in my soul. I will benefit from all these invaluable trainings for the rest of my life.

I would also like to thank all my past and current colleagues, Daniel Tornero, Emanuela Monni, Giedre Miskinyte, Marita Grønning Hansen, Linda Jansson, Cecilia Laterza, Somsak Wattananit, Katie Chapman, Zhaolu Wang, Andreas Arvidsson, James Wood, Marco Ledri, Karthikeyan Devaraju, Jemal Tatarishvili, Camilla Ekenstierna, Tamar Memanishvili, Masao Hirota, Koichi Oki, Yutaka Mine, Teona Roschupkina, Zhi Ma, Henrik Ahlenius, Jonas Fritze, Isaac Canals Montferrer, Aurélie Ginisty, Ella Quist, Matti Lam, Katarina Turesson, Susanne Jonsson, Deepti Chugh, My Andersson, Natalia Avaliani, Fredrik Berglind, Christine Ekdahl, Merab Kokaia, Bengt Mattsson, all members of the Lund stem cell center family and B10 family, for their generous help and kind accompany. Special thanks to Alexander Kertser, Kuti Baruch and Professor Michal Schwartz, for their valuable advice in the choroid plexus project.

Thank you all, I will cherish the nice days spent together forever.

Never give up hoping and endeavoring for the best results!

References

Arvidsson, A., T. Collin, D. Kirik, Z. Kokaia, and O. Lindvall. 2002. Neuronal replacement from endogenous precursors in the adult brain after stroke. *Nat Med* 8:963-970.

Avaliani, N., A.T. Sorensen, M. Ledri, J. Bengzon, P. Koch, O. Brustle, K. Deisseroth, M. Andersson, and M. Kokaia. 2014. Optogenetics reveal delayed afferent synaptogenesis on grafted human-induced pluripotent stem cell-derived neural progenitors. *Stem Cells* 32:3088-3098.

Baruch, K., A. Deczkowska, N. Rosenzweig, A. Tsitsou-Kampeli, A.M. Sharif, O. Matcovitch-Natan, A. Kertser, E. David, I. Amit, and M. Schwartz. 2016. PD-1 immune checkpoint blockade reduces pathology and improves memory in mouse models of Alzheimer's disease. *Nat Med* 22:135-137.

Carmichael, S.T., I. Archibeque, L. Luke, T. Nolan, J. Momiy, and S. Li. 2005. Growth-associated gene expression after stroke: evidence for a growth-promoting region in peri-infarct cortex. *Exp Neurol* 193:291-311.

Carmichael, S.T., L. Wei, C.M. Rovainen, and T.A. Woolsey. 2001. New patterns of intracortical projections after focal cortical stroke. *Neurobiol Dis* 8:910-922.

Cash, D., A.C. Easton, M. Mesquita, J. Beech, S. Williams, A. Lloyd, E. Irving, and S.C. Cramer. 2016. GSK249320, A Monoclonal Antibody Against the Axon Outgrowth Inhibition Molecule Myelin-Associated Glycoprotein, Improves Outcome of Rodents with Experimental Stroke. *Journal of neurology and experimental neuroscience* 2:28-33.

Cheng, Z., D.B. Bosco, L. Sun, X. Chen, Y. Xu, W. Tai, R. Didier, J. Li, J. Fan, X. He, and Y. Ren. 2017. Neural Stem Cell-Conditioned Medium Suppresses Inflammation and Promotes Spinal Cord Injury Recovery. *Cell Transplant* 26:469-482.

Chernykh, E.R., E.Y. Shevela, N.M. Starostina, S.A. Morozov, M.N. Davydova, E.V. Menyaeva, and A.A. Ostanin. 2016. Safety and Therapeutic Potential of M2 Macrophages in Stroke Treatment. *Cell Transplant* 25:1461-1471.

Covacu, R., C. Perez Estrada, L. Arvidsson, M. Svensson, and L. Brundin. 2014. Change of fate commitment in adult neural progenitor cells subjected to chronic inflammation. *J Neurosci* 34:11571-11582.

Cusimano, M., D. Biziato, E. Brambilla, M. Donega, C. Alfaro-Cervello, S. Snider, G. Salani, F. Pucci, G. Comi, J.M. Garcia-Verdugo, M. De Palma, G. Martino, and S. Pluchino. 2012. Transplanted neural stem/precursor cells instruct phagocytes and reduce secondary tissue damage in the injured spinal cord. *Brain* 135:447-460.

Daadi, M.M., A.L. Maag, and G.K. Steinberg. 2008. Adherent self-renewable human embryonic stem cell-derived neural stem cell line: functional engraftment in experimental stroke model. *PLoS One* 3:e1644.

Darsalia, V., U. Heldmann, O. Lindvall, and Z. Kokaia. 2005. Stroke-induced neurogenesis in aged brain. *Stroke* 36:1790-1795.

Darsalia, V., T. Kallur, and Z. Kokaia. 2007. Survival, migration and neuronal differentiation of human fetal striatal and cortical neural stem cells grafted in stroke-damaged rat striatum. *Eur J Neurosci* 26:605-614.

del Zoppo, G.J., G.W. Schmid-Schonbein, E. Mori, B.R. Copeland, and C.M. Chang. 1991. Polymorphonuclear leukocytes occlude capillaries following middle cerebral artery occlusion and reperfusion in baboons. *Stroke* 22:1276-1283.

Desestret, V., A. Riou, F. Chauveau, T.H. Cho, E. Devillard, M. Marinescu, R. Ferrera, C. Rey, M. Chanal, D. Angoulvant, J. Honnorat, N. Nighoghossian, Y. Berthezene, S. Nataf, and M. Wiart. 2013. In vitro and in vivo models of cerebral ischemia show discrepancy in therapeutic effects of M2 macrophages. *PLoS One* 8:e67063.

Dowd, E., C. Monville, E.M. Torres, and S.B. Dunnett. 2005. The Corridor Task: a simple test of lateralised response selection sensitive to unilateral dopamine deafferentation and graft-derived dopamine replacement in the striatum. *Brain Res Bull* 68:24-30.

Dull, T., R. Zufferey, M. Kelly, R.J. Mandel, M. Nguyen, D. Trono, and L. Naldini. 1998. A third-generation lentivirus vector with a conditional packaging system. *Journal of virology* 72:8463-8471.

Einstein, O., N. Grigoriadis, R. Mizrachi-Kol, E. Reinhartz, E. Polyzoidou, I. Lavon, I. Milonas, D. Karussis, O. Abramsky, and T. Ben-Hur. 2006. Transplanted neural precursor cells reduce brain inflammation to attenuate chronic experimental autoimmune encephalomyelitis. *Exp Neurol* 198:275-284.

Enlimomab Acute Stroke Trial Investigators. 2001. Use of anti-ICAM-1 therapy in ischemic stroke: results of the Enlimomab Acute Stroke Trial. In Neurology. 1428-1434.

Espuny-Camacho, I., K.A. Michelsen, D. Gall, D. Linaro, A. Hasche, J. Bonnefont, C. Bali, D. Orduz, A. Bilheu, A. Herpoel, N. Lambert, N. Gaspard, S. Peron, S.N. Schiffmann, M. Giugliano, A. Gaillard, and P. Vanderhaeghen. 2013. Pyramidal neurons derived from human pluripotent stem cells integrate efficiently into mouse brain circuits in vivo. *Neuron* 77:440-456.

Feng, X., D. Weng, F. Zhou, Y.D. Owen, H. Qin, J. Zhao, WenYu, Y. Huang, J. Chen, H. Fu, N. Yang, D. Chen, J. Li, R. Tan, and P. Shen. 2016. Activation of PPARgamma by a Natural Flavonoid Modulator, Apigenin Ameliorates Obesity-Related Inflammation Via Regulation of Macrophage Polarization. *EBioMedicine* 9:61-76.

Gao, J., R.J. Grill, T.J. Dunn, S. Bedi, J.A. Labastida, R.A. Hetz, H. Xue, J.R. Thonhoff, D.S. DeWitt, D.S. Prough, C.S. Cox, Jr., and P. Wu. 2016. Human Neural Stem Cell Transplantation-Mediated Alteration of Microglial/Macrophage Phenotypes after Traumatic Brain Injury. *Cell Transplant*

Gao, M., Q. Dong, H. Yao, Y. Lu, X. Ji, M. Zou, Z. Yang, M. Xu, and R. Xu. 2017. Systemic Administration of Induced Neural Stem Cells Regulates Complement Activation in Mouse Closed Head Injury Models. *Scientific reports* 7:45989.

Gomez-Nicola, D., B. Valle-Argos, N. Pallas-Bazarra, and M. Nieto-Sampedro. 2011. Interleukin-15 regulates proliferation and self-renewal of adult neural stem cells. *Mol Biol Cell* 22:1960-1970.

Gordon, S., and P.R. Taylor. 2005. Monocyte and macrophage heterogeneity. *Nat Rev Immunol* 5:953-964.
Grealish, S., B. Mattsson, P. Draxler, and A. Bjorklund. 2010. Characterisation of behavioural and neurodegenerative changes induced by intranigral 6-hydroxydopamine lesions in a mouse model of Parkinson's disease. *Eur J Neurosci* 31:2266-2278.
Han, Q., Q. Lin, P. Huang, M. Chen, X. Hu, H. Fu, S. He, F. Shen, H. Zeng, and Y. Deng. 2017. Microglia-derived IL-1beta contributes to axon development disorders and synaptic deficit through p38-MAPK signal pathway in septic neonatal rats. *J Neuroinflammation* 14:52.
Hess, D.C., L.R. Wechsler, W.M. Clark, S.I. Savitz, G.A. Ford, D. Chiu, D.R. Yavagal, K. Uchino, D.S. Liebeskind, A.P. Auchus, S. Sen, C.A. Sila, J.D. Vest, and R.W. Mays. 2017. Safety and efficacy of multipotent adult progenitor cells in acute ischaemic stroke (MASTERS): a randomised, double-blind, placebo-controlled, phase 2 trial. *Lancet Neurol* 16:360-368.
Hill, J.J., K. Jin, X.O. Mao, L. Xie, and D.A. Greenberg. 2012. Intracerebral chondroitinase ABC and heparan sulfate proteoglycan glypican improve outcome from chronic stroke in rats. *Proc Natl Acad Sci U S A* 109:9155-9160.
Hodics, T., L.G. Cohen, and S.C. Cramer. 2006. Functional imaging of intervention effects in stroke motor rehabilitation. *Archives of physical medicine and rehabilitation* 87:S36-42.
Honmou, O., K. Houkin, T. Matsunaga, Y. Niitsu, S. Ishiai, R. Onodera, S.G. Waxman, and J.D. Kocsis. 2011. Intravenous administration of auto serum-expanded autologous mesenchymal stem cells in stroke. *Brain* 134:1790-1807.
Hou, S.W., Y.Q. Wang, M. Xu, D.H. Shen, J.J. Wang, F. Huang, Z. Yu, and F.Y. Sun. 2008. Functional integration of newly generated neurons into striatum after cerebral ischemia in the adult rat brain. *Stroke* 39:2837-2844.
Hu, X., P. Li, Y. Guo, H. Wang, R.K. Leak, S. Chen, Y. Gao, and J. Chen. 2012. Microglia/macrophage polarization dynamics reveal novel mechanism of injury expansion after focal cerebral ischemia. *Stroke* 43:3063-3070.
Iadecola, C., and J. Anrather. 2011. The immunology of stroke: from mechanisms to translation. *Nat Med* 17:796-808.
Ishibashi, S., M. Sakaguchi, T. Kuroiwa, M. Yamasaki, Y. Kanemura, I. Shizuko, T. Shimazaki, M. Onodera, H. Okano, and H. Mizusawa. 2004. Human neural stem/progenitor cells, expanded in long-term neurosphere culture, promote functional recovery after focal ischemia in Mongolian gerbils. *Journal of neuroscience research* 78:215-223.
Jakubs, K., S. Bonde, R.E. Iosif, C.T. Ekdahl, Z. Kokaia, M. Kokaia, and O. Lindvall. 2008. Inflammation regulates functional integration of neurons born in adult brain. *J Neurosci* 28:12477-12488.
Jin, K., X. Wang, L. Xie, X.O. Mao, and D.A. Greenberg. 2010. Transgenic ablation of doublecortin-expressing cells suppresses adult neurogenesis and worsens stroke outcome in mice. *Proc Natl Acad Sci U S A* 107:7993-7998.
Kalladka, D., J. Sinden, K. Pollock, C. Haig, J. McLean, W. Smith, A. McConnachie, C. Santosh, P.M. Bath, L. Dunn, and K.W. Muir. 2016. Human neural stem cells in

patients with chronic ischaemic stroke (PISCES): a phase 1, first-in-man study. *Lancet* 388:787-796.
Kelly, S., T.M. Bliss, A.K. Shah, G.H. Sun, M. Ma, W.C. Foo, J. Masel, M.A. Yenari, I.L. Weissman, N. Uchida, T. Palmer, and G.K. Steinberg. 2004. Transplanted human fetal neural stem cells survive, migrate, and differentiate in ischemic rat cerebral cortex. *Proc Natl Acad Sci U S A* 101:11839-11844.
Kim, D.Y., S.H. Park, S.U. Lee, D.H. Choi, H.W. Park, S.H. Paek, H.Y. Shin, E.Y. Kim, S.P. Park, and J.H. Lim. 2007. Effect of human embryonic stem cell-derived neuronal precursor cell transplantation into the cerebral infarct model of rat with exercise. *Neuroscience research* 58:164-175.
Kim, J.E., M.L. O'Sullivan, C.A. Sanchez, M. Hwang, M.A. Israel, K. Brennand, T.J. Deerinck, L.S. Goldstein, F.H. Gage, M.H. Ellisman, and A. Ghosh. 2011. Investigating synapse formation and function using human pluripotent stem cell-derived neurons. *Proc Natl Acad Sci U S A* 108:3005-3010.
Koch, P., T. Opitz, J.A. Steinbeck, J. Ladewig, and O. Brustle. 2009. A rosette-type, self-renewing human ES cell-derived neural stem cell with potential for in vitro instruction and synaptic integration. *Proc Natl Acad Sci U S A* 106:3225-3230.
Kokaia, Z., G. Martino, M. Schwartz, and O. Lindvall. 2012. Cross-talk between neural stem cells and immune cells: the key to better brain repair? *Nature neuroscience* 15:1078-1087.
Krams, M., K.R. Lees, W. Hacke, A.P. Grieve, J.M. Orgogozo, and G.A. Ford. 2003. Acute Stroke Therapy by Inhibition of Neutrophils (ASTIN): an adaptive dose-response study of UK-279,276 in acute ischemic stroke. *Stroke* 34:2543-2548.
Li, S., E.H. Nie, Y. Yin, L.I. Benowitz, S. Tung, H.V. Vinters, F.R. Bahjat, M.P. Stenzel-Poore, R. Kawaguchi, G. Coppola, and S.T. Carmichael. 2015. GDF10 is a signal for axonal sprouting and functional recovery after stroke. *Nature neuroscience* 18:1737-1745.
Lindau, N.T., B.J. Banninger, M. Gullo, N.A. Good, L.C. Bachmann, M.L. Starkey, and M.E. Schwab. 2014. Rewiring of the corticospinal tract in the adult rat after unilateral stroke and anti-Nogo-A therapy. *Brain* 137:739-756.
Liu, L., and K. Duff. 2008. A technique for serial collection of cerebrospinal fluid from the cisterna magna in mouse. *J Vis Exp*
Liu, Q., N. Sanai, W.N. Jin, A. La Cava, L. Van Kaer, and F.D. Shi. 2016a. Neural stem cells sustain natural killer cells that dictate recovery from brain inflammation. *Nature neuroscience* 19:243-252.
Liu, X., J. Liu, S. Zhao, H. Zhang, W. Cai, M. Cai, X. Ji, R.K. Leak, Y. Gao, J. Chen, and X. Hu. 2016b. Interleukin-4 Is Essential for Microglia/Macrophage M2 Polarization and Long-Term Recovery After Cerebral Ischemia. *Stroke* 47:498-504.
Magnusson, J.P., C. Goritz, J. Tatarishvili, D.O. Dias, E.M. Smith, O. Lindvall, Z. Kokaia, and J. Frisen. 2014. A latent neurogenic program in astrocytes regulated by Notch signaling in the mouse. *Science* 346:237-241.
Mantovani, A., S.K. Biswas, M.R. Galdiero, A. Sica, and M. Locati. 2013. Macrophage plasticity and polarization in tissue repair and remodelling. *J Pathol* 229:176-185.

Marti-Fabregas, J., M. Romaguera-Ros, U. Gomez-Pinedo, S. Martinez-Ramirez, R.M.E. Jimenez-Xarrie, J.L.M.-V. R, and J.M. Garcia-Verdugo. 2010. Proliferation in the human ipsilateral subventricular zone after ischemic stroke: Neurology 2010;Vol.74:357-365. *Ann Neurosci* 17:134-135.

Michelsen, K.A., S. Acosta-Verdugo, M. Benoit-Marand, I. Espuny-Camacho, N. Gaspard, B. Saha, A. Gaillard, and P. Vanderhaeghen. 2015. Area-specific reestablishment of damaged circuits in the adult cerebral cortex by cortical neurons derived from mouse embryonic stem cells. *Neuron* 85:982-997.

Mine, Y., J. Tatarishvili, K. Oki, E. Monni, Z. Kokaia, and O. Lindvall. 2013. Grafted human neural stem cells enhance several steps of endogenous neurogenesis and improve behavioral recovery after middle cerebral artery occlusion in rats. *Neurobiol Dis* 52:191-203.

Minger, S.L., A. Ekonomou, E.M. Carta, A. Chinoy, R.H. Perry, and C.G. Ballard. 2007. Endogenous neurogenesis in the human brain following cerebral infarction. *Regen Med* 2:69-74.

Miro-Mur, F., I. Perez-de-Puig, M. Ferrer-Ferrer, X. Urra, C. Justicia, A. Chamorro, and A.M. Planas. 2016. Immature monocytes recruited to the ischemic mouse brain differentiate into macrophages with features of alternative activation. *Brain Behav Immun* 53:18-33.

Moskowitz, M.A., E.H. Lo, and C. Iadecola. 2010. The science of stroke: mechanisms in search of treatments. *Neuron* 67:181-198.

Mosser, C.A., S. Baptista, I. Arnoux, and E. Audinat. 2017. Microglia in CNS development: Shaping the brain for the future. *Progress in neurobiology* 149-150:1-20.

Muneton-Gomez, V.C., E. Doncel-Perez, A.P. Fernandez, J. Serrano, A. Pozo-Rodrigalvarez, L. Vellosillo-Huerta, J.S. Taylor, G.P. Cardona-Gomez, M. Nieto-Sampedro, and R. Martinez-Murillo. 2012. Neural differentiation of transplanted neural stem cells in a rat model of striatal lacunar infarction: light and electron microscopic observations. *Frontiers in cellular neuroscience* 6:30.

Oki, K., J. Tatarishvili, J. Wood, P. Koch, S. Wattananit, Y. Mine, E. Monni, D. Tornero, H. Ahlenius, J. Ladewig, O. Brustle, O. Lindvall, and Z. Kokaia. 2012. Human-induced pluripotent stem cells form functional neurons and improve recovery after grafting in stroke-damaged brain. *Stem Cells* 30:1120-1133.

Osakada, F., and E.M. Callaway. 2013. Design and generation of recombinant rabies virus vectors. *Nature protocols* 8:1583-1601.

Perez-de Puig, I., F. Miro, A. Salas-Perdomo, E. Bonfill-Teixidor, M. Ferrer-Ferrer, L. Marquez-Kisinousky, and A.M. Planas. 2013. IL-10 deficiency exacerbates the brain inflammatory response to permanent ischemia without preventing resolution of the lesion. *J Cereb Blood Flow Metab* 33:1955-1966.

Rahpeymai, Y., M.A. Hietala, U. Wilhelmsson, A. Fotheringham, I. Davies, A.K. Nilsson, J. Zwirner, R.A. Wetsel, C. Gerard, M. Pekny, and M. Pekna. 2006. Complement: a novel factor in basal and ischemia-induced neurogenesis. *EMBO J* 25:1364-1374.

Robel, S., B. Berninger, and M. Gotz. 2011. The stem cell potential of glia: lessons from reactive gliosis. *Nat Rev Neurosci* 12:88-104.

Robin, A.M., Z.G. Zhang, L. Wang, R.L. Zhang, M. Katakowski, L. Zhang, Y. Wang, C. Zhang, and M. Chopp. 2006. Stromal cell-derived factor 1alpha mediates neural progenitor cell motility after focal cerebral ischemia. *J Cereb Blood Flow Metab* 26:125-134.

Sansone, M., C. Castellano, S. Palazzesi, M. Battaglia, and M. Ammassari-Teule. 1993. Effects of oxiracetam, physostigmine, and their combination on active and passive avoidance learning in mice. *Pharmacol Biochem Behav* 44:451-455.

Schaechter, J.D., E. Kraft, T.S. Hilliard, R.M. Dijkhuizen, T. Benner, S.P. Finklestein, B.R. Rosen, and S.C. Cramer. 2002. Motor recovery and cortical reorganization after constraint-induced movement therapy in stroke patients: a preliminary study. *Neurorehabilitation and neural repair* 16:326-338.

Scholzke, M.N., A. Rottinger, S. Murikinati, N. Gehrig, C. Leib, and M. Schwaninger. 2011. TWEAK regulates proliferation and differentiation of adult neural progenitor cells. *Mol Cell Neurosci* 46:325-332.

Shechter, R., O. Miller, G. Yovel, N. Rosenzweig, A. London, J. Ruckh, K.W. Kim, E. Klein, V. Kalchenko, P. Bendel, S.A. Lira, S. Jung, and M. Schwartz. 2013. Recruitment of beneficial M2 macrophages to injured spinal cord is orchestrated by remote brain choroid plexus. *Immunity* 38:555-569.

Silver, J., and J.H. Miller. 2004. Regeneration beyond the glial scar. *Nat Rev Neurosci* 5:146-156.

Steinberg, G.K., D. Kondziolka, L.R. Wechsler, L.D. Lunsford, M.L. Coburn, J.B. Billigen, A.S. Kim, J.N. Johnson, D. Bates, B. King, C. Case, M. McGrogan, E.W. Yankee, and N.E. Schwartz. 2016. Clinical Outcomes of Transplanted Modified Bone Marrow-Derived Mesenchymal Stem Cells in Stroke: A Phase 1/2a Study. *Stroke* 47:1817-1824.

Suarez-Monteagudo, C., P. Hernandez-Ramirez, L. Alvarez-Gonzalez, I. Garcia-Maeso, K. de la Cuetara-Bernal, L. Castillo-Diaz, M.L. Bringas-Vega, G. Martinez-Aching, L.M. Morales-Chacon, M.M. Baez-Martin, C. Sanchez-Catasus, M. Carballo-Barreda, R. Rodriguez-Rojas, L. Gomez-Fernandez, E. Alberti-Amador, C. Macias-Abraham, E.D. Balea, L.C. Rosales, L. Del Valle Perez, B.B. Ferrer, R.M. Gonzalez, and J.A. Bergado. 2009. Autologous bone marrow stem cell neurotransplantation in stroke patients. An open study. *Restorative neurology and neuroscience* 27:151-161.

Taguchi, A., T. Soma, H. Tanaka, T. Kanda, H. Nishimura, H. Yoshikawa, Y. Tsukamoto, H. Iso, Y. Fujimori, D.M. Stern, H. Naritomi, and T. Matsuyama. 2004. Administration of CD34+ cells after stroke enhances neurogenesis via angiogenesis in a mouse model. *J Clin Invest* 114:330-338.

Takahashi, K., K. Tanabe, M. Ohnuki, M. Narita, T. Ichisaka, K. Tomoda, and S. Yamanaka. 2007. Induction of pluripotent stem cells from adult human fibroblasts by defined factors. *Cell* 131:861-872.

Thored, P., A. Arvidsson, E. Cacci, H. Ahlenius, T. Kallur, V. Darsalia, C.T. Ekdahl, Z. Kokaia, and O. Lindvall. 2006. Persistent production of neurons from adult brain stem cells during recovery after stroke. *Stem Cells* 24:739-747.

Thored, P., U. Heldmann, W. Gomes-Leal, R. Gisler, V. Darsalia, J. Taneera, J.M. Nygren, S.E. Jacobsen, C.T. Ekdahl, Z. Kokaia, and O. Lindvall. 2009. Long-term

accumulation of microglia with proneurogenic phenotype concomitant with persistent neurogenesis in adult subventricular zone after stroke. *Glia* 57:835-849.

Tornero, D., S. Wattananit, M. Gronning Madsen, P. Koch, J. Wood, J. Tatarishvili, Y. Mine, R. Ge, E. Monni, K. Devaraju, R.F. Hevner, O. Brustle, O. Lindvall, and Z. Kokaia. 2013. Human induced pluripotent stem cell-derived cortical neurons integrate in stroke-injured cortex and improve functional recovery. *Brain* 136:3561-3577.

Wattananit, S., D. Tornero, N. Graubardt, T. Memanishvili, E. Monni, J. Tatarishvili, G. Miskinyte, R. Ge, H. Ahlenius, O. Lindvall, M. Schwartz, and Z. Kokaia. 2016. Monocyte-Derived Macrophages Contribute to Spontaneous Long-Term Functional Recovery after Stroke in Mice. *J Neurosci* 36:4182-4195.

West, M.J., L. Slomianka, and H.J. Gundersen. 1991. Unbiased stereological estimation of the total number of neurons in thesubdivisions of the rat hippocampus using the optical fractionator. *The Anatomical record* 231:482-497.

Yan, Y.P., K.A. Sailor, B.T. Lang, S.W. Park, R. Vemuganti, and R.J. Dempsey. 2007. Monocyte chemoattractant protein-1 plays a critical role in neuroblast migration after focal cerebral ischemia. *J Cereb Blood Flow Metab* 27:1213-1224.

Yan, Y.P., K.A. Sailor, R. Vemuganti, and R.J. Dempsey. 2006. Insulin-like growth factor-1 is an endogenous mediator of focal ischemia-induced neural progenitor proliferation. *Eur J Neurosci* 24:45-54.

Zhang, K., J. Zheng, G. Bian, L. Liu, Q. Xue, F. Liu, C. Yu, H. Zhang, B. Song, S.K. Chung, G. Ju, and J. Wang. 2015. Polarized Macrophages Have Distinct Roles in the Differentiation and Migration of Embryonic Spinal-cord-derived Neural Stem Cells After Grafting to Injured Sites of Spinal Cord. *Molecular therapy : the journal of the American Society of Gene Therapy* 23:1077-1091.

Zhao, L.R., W.M. Duan, M. Reyes, C.D. Keene, C.M. Verfaillie, and W.C. Low. 2002. Human bone marrow stem cells exhibit neural phenotypes and ameliorate neurological deficits after grafting into the ischemic brain of rats. *Exp Neurol* 174:11-20.

Zheng, W., R.S. Nowakowski, and F.M. Vaccarino. 2004. Fibroblast growth factor 2 is required for maintaining the neural stem cell pool in the mouse brain subventricular zone. *Dev Neurosci* 26:181-196.

Ziv, Y., H. Avidan, S. Pluchino, G. Martino, and M. Schwartz. 2006. Synergy between immune cells and adult neural stem/progenitor cells promotes functional recovery from spinal cord injury. *Proc Natl Acad Sci U S A* 103:13174-13179.

Appendix